Second-order two-scale analysis and numerical algorithms for the hyperbolic–parabolic equations with rapidly oscillating coefficients*

Dong Hao(董 灏)[a], Nie Yu-Feng(聂玉峰)[a]†, Cui Jun-Zhi(崔俊芝)[b], and Wu Ya-Tao(武亚涛)[a]

[a] School of Science, Northwestern Polytechnical University, Xi'an 710129, China
[b] Academy of Mathematics and Systems Science, Chinese Academy of Sciences, Beijing 100190, China

(Received 15 March 2015; revised manuscript received 22 April 2015; published online 10 August 2015)

We study the hyperbolic–parabolic equations with rapidly oscillating coefficients. The formal second-order two-scale asymptotic expansion solutions are constructed by the multiscale asymptotic analysis. In addition, we theoretically explain the importance of the second-order two-scale solution by the error analysis in the pointwise sense. The associated explicit convergence rates are also obtained. Then a second-order two-scale numerical method based on the Newmark scheme is presented to solve the equations. Finally, some numerical examples are used to verify the effectiveness and efficiency of the multiscale numerical algorithm we proposed.

Keywords: hyperbolic–parabolic equations, rapidly oscillating coefficients, second-order two-scale numerical method, Newmark scheme

PACS: 02.30.Jr, 02.60.Cb **DOI:** 10.1088/1674-1056/24/9/090204

1. Introduction

In recent years, composite materials have been widely used in engineering applications owing to their attractive physical and mechanical properties. Due to large heterogeneities (caused by inclusions or holes) in the composite structures (see Fig. 1 for example), the direct numerical computation of the composite materials needs a huge amount of computational resources and a prohibitive amount of computational time because it requires a very fine mesh to capture the micro-scale behavior. Fortunately, mathematicians and engineers have developed some multiscale methods to solve this difficult problem in the past thirty years, such as the asymptotic homogenization method (AHM), heterogeneous multiscale method (HMM), variational multiscale method (VMS), and multiscale finite element method (MSFEM). We refer the interested readers to Ref. [1] for the details. The basic idea of the homogenization method is to give the global equivalent behavior of the composite structure by smoothing the micro-scale fluctuations due to the heterogeneities. However, small periodic parameter ε, while small, often does not reach zero in many engineering applications. At this time, the numerical accuracy of the standard homogenization method may not meet the actual need (see Refs. [2]–[11]). To this end, multiscale asymptotic methods and associated numerical algorithms are developed to capture the microscopic properties of the composite materials. The main idea of the multiscale asymptotic methods is to add corrector terms to the homogenized solution (see Refs. [2]–[11]).

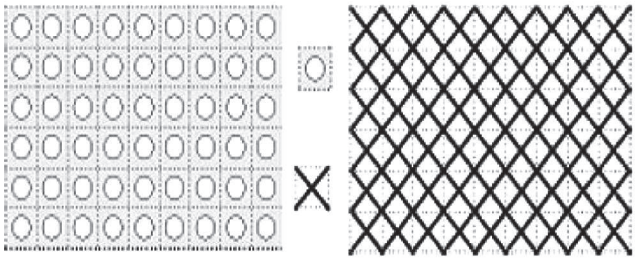


Fig. 1. The whole domain Ω and the unit cell Y.[1]

To the best of our knowledge, hyperbolic–parabolic equations with rapidly oscillating coefficients have a wide range of practical applications in composite structures, which describe the wave scattering and diffraction with damping in a heterogeneous medium (see Refs. [12]–[14]). In addition, the hyperbolic–parabolic equations are the model equations of nonclassical heat conduction problems under the ultra conventional heating (cooling) condition. This model is widely used in the fields of micro-electro-mechanical systems, laser, and aerospace technology (see Ref. [15]). Therefore, it is significant to study the hyperbolic–parabolic equations with rapidly oscillating coefficients. The homogenization of the linear hyperbolic–parabolic equations in the perforated domains can be found in Ref. [12]. In addition, an asymptotic analysis for a weakly damped wave equation in an elastic problem can be found in Ref. [13]. The author proved a homogenization theorem for the weakly damped wave equation. Besides, the authors in Ref. [16] analyzed the effective behavior of the solution of a wave equation with interior and boundary damp-

*Project supported by the National Natural Science Foundation of China (Grant No. 11471262), the National Basic Research Program of China (Grant No. 2012CB025904), and the State Key Laboratory of Science and Engineering Computing and the Center for High Performance Computing of Northwestern Polytechnical University, China.

†Corresponding author. E-mail: yfnie@nwpu.edu.cn

© 2015 Chinese Physical Society and IOP Publishing Ltd

ing defined in a periodical perforated medium. The analysis of this problem is more difficult than that in Ref. [12]. Moreover, the homogenization of the weakly damped nonlinear hyperbolic–parabolic equations was studied in Ref. [17]. The author proved that the solutions of a class of highly oscillatory nonlinear evolution problems converge to the solution of a homogenized quasilinear hyperbolic–parabolic problem based on the sigma-convergence method. On the other hand, there is much literature focusing on the concern weighted (in time) and pointwise (in time) energy decay estimates of the damped wave equations (see Refs. [14] and [18]–[20]). In summary, the current research on the hyperbolic–parabolic equation with damping mainly focuses on the homogenized analysis and the energy decay estimates.

In this paper, we focus on the second-order two-scale analysis for the hyperbolic–parabolic equations with rapidly oscillating coefficients in order to capture the micro-scale behavior. To our knowledge, it is difficult to obtain the explicit convergence rate for the wave equation with non-homogeneous boundary condition, because it is extremely difficult to obtain explicitly a prior estimate of the solution (see Refs. [6] and [7]). Therefore, obtaining the explicit convergence rate for the hyperbolic–parabolic equation will be a more difficult problem. The main idea of this paper is to impose the homogeneous Dirichlet boundary conditions on the auxiliary cell problems (see Refs. [4]–[10]). If Ω is the union of the entire periodic cells, the second-order two-scale solution of problem (1) will satisfy automatically the boundary conditions on $\partial\Omega$. In this case, we can obtain the explicit convergence rate and improve the error estimate order of the second-order two-scale solution under some extra assumptions. The main result of this paper is Theorems 3 and 4 in Section 3. Surprisingly, the error estimate of the hyperbolic–parabolic equations can devolve back to the error estimate of the hyperbolic equation.

This paper is organized as follows. In Section 2, the detailed construction of the second-order two-scale solution to the hyperbolic–parabolic equations is given by multiscale asymptotic analysis. In addition, we give the error analysis in the pointwise sense of first-order two-scale solution and second-order two-scale solution. Through the above analysis, we theoretically explain the importance of the second-order solution in capturing the micro-scale oscillating information. In Section 3, we derive the explicit convergence order of the second-order two-scale solution. From the convergence results, we can easily obtain the convergence conclusion for the hyperbolic equation. In Section 4, we give the finite element approximation schemes for the auxiliary cell problems and the homogenization problem of the hyperbolic–parabolic equations. After that, we present a second-order two-scale numerical method to solve the hyperbolic–parabolic equations based on the Newmark scheme (see Ref. [21]) and the average technique (see Ref. [2]), and give a detailed comparison and analysis of the computational efficiency and stability between the second-order two-scale method and the direct finite element method. In Section 5, some numerical examples are given, which illustrate our method. Finally, the conclusions are given in Section 6.

For convenience,we use the Einstein summation convention on repeated indices in this paper.

2. Governing equations and multiscale asymptotic analysis

Consider the initial-boundary value problems of the hyperbolic–parabolic equations with rapidly oscillating coefficients as follows:

$$\begin{cases} \rho^{\varepsilon}(\boldsymbol{x},t)\dfrac{\partial^2 u^{\varepsilon}(\boldsymbol{x},t)}{\partial t^2}+\mu^{\varepsilon}(\boldsymbol{x},t)\dfrac{\partial u^{\varepsilon}(\boldsymbol{x},t)}{\partial t} \\ =\dfrac{\partial}{\partial x_i}\left(a_{ij}^{\varepsilon}(\boldsymbol{x},t)\dfrac{\partial u^{\varepsilon}(\boldsymbol{x},t)}{\partial x_j}\right) \\ \quad +f(\boldsymbol{x},t), \quad (\boldsymbol{x},t)\in\Omega\times(0,T), \\ u^{\varepsilon}(\boldsymbol{x},t)=\phi(\boldsymbol{x},t), \quad (\boldsymbol{x},t)\in\partial\Omega\times(0,T), \\ u^{\varepsilon}(\boldsymbol{x},0)=u^0(\boldsymbol{x}), \quad \left.\dfrac{\partial u^{\varepsilon}(\boldsymbol{x},t)}{\partial t}\right|_{t=0}=u^1(\boldsymbol{x}), \quad \boldsymbol{x}\in\Omega, \end{cases} \tag{1}$$

where Ω is a bounded convex domain in $\mathbb{R}^n (n=2,3)$ with a boundary $\partial\Omega$, and $f(\boldsymbol{x},t),\phi(\boldsymbol{x},t),u^0(\boldsymbol{x}),u^1(\boldsymbol{x})$ are given functions. The coefficient $\rho^{\varepsilon}(\boldsymbol{x},t)$ and the matrix $a_{ij}^{\varepsilon}(\boldsymbol{x},t)$ describe the physical property of the material, and $\mu^{\varepsilon}(\boldsymbol{x},t)$ is the dissipation damping coefficient (see Ref. [12]).

At first, we set $\boldsymbol{y}=\boldsymbol{x}/\varepsilon$ and make the following hypothesis to obtain a series of conclusions:

$$\text{(A)}\quad \begin{cases} a_{ij}^{\varepsilon}=a_{ji}^{\varepsilon}, \\ \exists\gamma_0,\gamma_1>0, \gamma_0|\xi|^2\le a_{ij}^{\varepsilon}\xi_i\xi_j\le\gamma_1|\xi|^2, \\ \forall\xi=(\xi_1,\xi_2,\ldots,\xi_n)\in\mathbb{R}^n, \\ a_{ij}^{\varepsilon} \text{ are } 1-\text{periodic functions in } \boldsymbol{y}; \end{cases}$$

$$\text{(B)}\quad \begin{cases} \rho^{\varepsilon}\in L^{\infty}(\Omega\times[0,T]), \mu^{\varepsilon}\in L^{\infty}(\Omega\times[0,T]), \\ 0<\rho^0\le\rho^{\varepsilon}, \\ 0<\mu^0\le\mu^{\varepsilon}, \\ \rho^{\varepsilon} \text{ and } \mu^{\varepsilon} \text{ are } 1-\text{periodic functions in } \boldsymbol{y}; \end{cases}$$

$$\text{(C)}\quad f\in L^2(\Omega\times(0,T)), \quad \phi\in L^2(\Omega\times(0,T)), \quad u^0\in H^1(\Omega),\ u^1\in L^2(\Omega).$$

In this section, we first give the specific construction process of the first-order two-scale asymptotic solution and the second-order two-scale asymptotic solution to the problem (1). In order to save the length of article, we denote the first-order two-scale solution and the second-order two-scale solution as FOTS and SOTS, respectively. The error analysis in the pointwise sense of FOTS and SOTS is also given, which neatly illustrates the extreme necessity of SOTS. We analyze the error in the pointwise sense first because it will give the residual

equations which is of vital significance for error analysis in the integral sense.

2.1. Second-order two-scale analysis of the hyperbolic–parabolic equations

To the problem (1), we suppose that $u^{\varepsilon}(\boldsymbol{x},t)$ can be expressed in the following asymptotic form:

$$u^{\varepsilon}(\boldsymbol{x},t)=u^{(0)}(\boldsymbol{x},t)+\varepsilon u^{(1)}(\boldsymbol{x},t)+\varepsilon^2 u^{(2)}(\boldsymbol{x},t)+\cdots. \quad (2)$$

Due to $\boldsymbol{y}=\boldsymbol{x}/\varepsilon\in Y$ (Y is the unit cell, where $Y=(0,1)^n$, $n=2,3$), the chain rule can be denoted as $\frac{\partial}{\partial x_i}\to\frac{\partial}{\partial x_i}+\frac{1}{\varepsilon}\frac{\partial}{\partial y_i}$, then substituting Eq. (2) into Eq. (1) and matching terms of the same order of ε, we can immediately obtain

$$\begin{aligned}
&\varepsilon^{-2}\left[\frac{\partial}{\partial y_i}\left(a_{ij}(\boldsymbol{y},t)\frac{\partial u^{(0)}}{\partial y_j}\right)\right]+\varepsilon^{-1}\left[\frac{\partial}{\partial x_i}\left(a_{ij}(\boldsymbol{y},t)\frac{\partial u^{(0)}}{\partial y_j}\right)\right.\\
&\left.+\frac{\partial}{\partial y_i}\left(a_{ij}(\boldsymbol{y},t)\left(\frac{\partial u^{(0)}}{\partial x_j}+\frac{\partial u^{(1)}}{\partial y_j}\right)\right)\right]\\
&+\varepsilon^{0}\left[\frac{\partial}{\partial y_i}\left(a_{ij}(\boldsymbol{y},t)\left(\frac{\partial u^{(1)}}{\partial x_j}+\frac{\partial u^{(2)}}{\partial y_j}\right)\right)\right.\\
&\left.+\frac{\partial}{\partial x_i}\left(a_{ij}(\boldsymbol{y},t)\left(\frac{\partial u^{(0)}}{\partial x_j}+\frac{\partial u^{(1)}}{\partial y_j}\right)\right)+f\right]+\mathrm{O}(\varepsilon)\\
&=\rho(\boldsymbol{y},t)\left(\frac{\partial^2 u^{(0)}}{\partial t^2}+\varepsilon\frac{\partial^2 u^{(1)}}{\partial t^2}+\varepsilon^2\frac{\partial^2 u^{(2)}}{\partial t^2}+\cdots\right)\\
&+\mu(\boldsymbol{y},t)\left(\frac{\partial u^{(0)}}{\partial t}+\varepsilon\frac{\partial u^{(1)}}{\partial t}+\varepsilon^2\frac{\partial u^{(2)}}{\partial t}+\cdots\right). \quad (3)
\end{aligned}$$

After that, a series of equations are obtained if the coefficients of ε^i ($i=-2,-1,0,1,\ldots$) from both sides of Eq. (3) are set to be equal to each other, which are listed as follows:

$$\mathrm{O}(\varepsilon^{-2}):\ \frac{\partial}{\partial y_i}\left(a_{ij}(\boldsymbol{y},t)\frac{\partial u^{(0)}}{\partial y_j}\right)=0, \quad (4)$$

$$\begin{aligned}
\mathrm{O}(\varepsilon^{-1}):\ &\frac{\partial}{\partial x_i}\left(a_{ij}(\boldsymbol{y},t)\frac{\partial u^{(0)}}{\partial y_j}\right)\\
&+\frac{\partial}{\partial y_i}\left(a_{ij}(\boldsymbol{y},t)\left(\frac{\partial u^{(0)}}{\partial x_j}+\frac{\partial u^{(1)}}{\partial y_j}\right)\right)=0, \quad (5)
\end{aligned}$$

$$\begin{aligned}
\mathrm{O}(\varepsilon^{0}):\ &\rho(\boldsymbol{y},t)\frac{\partial^2 u^{(0)}}{\partial t^2}+\mu(\boldsymbol{y},t)\frac{\partial u^{(0)}}{\partial t}\\
&=\frac{\partial}{\partial y_i}\left(a_{ij}(\boldsymbol{y},t)\left(\frac{\partial u^{(1)}}{\partial x_j}+\frac{\partial u^{(2)}}{\partial y_j}\right)\right)\\
&+\frac{\partial}{\partial x_i}\left(a_{ij}(\boldsymbol{y},t)\left(\frac{\partial u^{(0)}}{\partial x_j}+\frac{\partial u^{(1)}}{\partial y_j}\right)\right)+f. \quad (6)
\end{aligned}$$

Now we solve the asymptotic expansion terms recursively. Firstly, applying the standard asymptotic homogenization theory to Eq. (4), we know that the first term of the asymptotic expansion (2) only depends on macroscopic scale $\boldsymbol{x}$, which can be expressed as $u^{(0)}=u^{(0)}(\boldsymbol{x},t)$.

Secondly, it can be easily recognized that equation (5) is linear with respect to $u^{(0)}$, so $u^{(1)}$ can be defined as

$$u^{(1)}=N^{\alpha_1}(\boldsymbol{y},t)\frac{\partial u^{(0)}(\boldsymbol{x},t)}{\partial x_{\alpha_1}},$$

where $N^{\alpha_1}(\boldsymbol{x},\boldsymbol{y},t)$ is the first-order auxiliary cell function defined in unit cell Y. Substituting $u^{(1)}$ into Eq. (5), we obtain the following equation with attaching boundary condition:

$$\begin{cases}
\dfrac{\partial}{\partial y_i}\left(a_{ij}(\boldsymbol{y},t)\dfrac{\partial N^{\alpha_1}(\boldsymbol{y},t)}{\partial y_j}\right)=-\dfrac{\partial a_{i\alpha_1}(\boldsymbol{y},t)}{\partial y_i},\\
(\boldsymbol{y},t)\in Y\times(0,T),\\
N^{\alpha_1}(\boldsymbol{y},t)=0,\quad (\boldsymbol{y},t)\in\partial Y\times(0,T).
\end{cases} \quad (7)$$

Remark 1 According to Lax–Milgram theorem and assumption (A) , it is easy to prove that problem (7) has the unique solution for any fixed time variable t.

Then, inspired by Refs. [7] and [11], we can be define the homogenized material coefficients $\hat{\rho}(t)$, $\hat{\mu}(t)$, and $\hat{a}_{ij}(t)$ as follows:

$$\begin{aligned}
\hat{\rho}(t)&=\frac{1}{|Y|}\int_Y\rho(\boldsymbol{y},t)\mathrm{d}Y,\\
\hat{\mu}(t)&=\frac{1}{|Y|}\int_Y\mu(\boldsymbol{y},t)\mathrm{d}Y,\\
\hat{a}_{ij}(t)&=\frac{1}{|Y|}\int_Y\left[a_{ij}(\boldsymbol{y},t)+a_{ik}(\boldsymbol{y},t)\frac{\partial N^j(\boldsymbol{y},t)}{\partial y_k}\right]\mathrm{d}Y. \quad (8)
\end{aligned}$$

Further, we can define the homogenized problem as follows:

$$\begin{cases}
\hat{\rho}(t)\dfrac{\partial^2 u^{(0)}(\boldsymbol{x},t)}{\partial t^2}+\hat{\mu}(t)\dfrac{\partial u^{(0)}(\boldsymbol{x},t)}{\partial t}\\
=\dfrac{\partial}{\partial x_i}\left(\hat{a}_{ij}(t)\dfrac{\partial u^{(0)}(\boldsymbol{x},t)}{\partial x_j}\right)+f(\boldsymbol{x},t),(\boldsymbol{x},t)\in\Omega\times(0,T),\\
u^{(0)}(\boldsymbol{x},t)=\phi(\boldsymbol{x},t),\quad (\boldsymbol{x},t)\in\partial\Omega\times(0,T),\\
u^{(0)}(\boldsymbol{x},0)=u^0(\boldsymbol{x}),\ \left.\dfrac{\partial u^{(0)}(\boldsymbol{x},t)}{\partial t}\right|_{t=0}=u^1(\boldsymbol{x}),\quad \boldsymbol{x}\in\Omega.
\end{cases} \quad (9)$$

Remark 2 Under assumptions (A) and (B), we can prove that the homogenized coefficient tensor $\hat{a}_{ij}(t)$ is symmetric, positive-definite, and bounded (see Ref. [7]). Besides, it is easy to prove that $\hat{\rho}(t)$ and $\hat{\mu}(t)$ are bounded. In addition, the homogenized problem (9) has a unique solution according to the conclusion in Ref. [12].

Finally, from Eqs. (6) and (9), the following equation is obtained:

$$\begin{aligned}
&\frac{\partial}{\partial y_i}\left(a_{ij}(\boldsymbol{y},t)\frac{\partial u^{(2)}}{\partial y_j}\right)\\
&=\rho(\boldsymbol{y},t)\frac{\partial^2 u^{(0)}}{\partial t^2}+\mu(\boldsymbol{y},t)\frac{\partial u^{(0)}}{\partial t}-\frac{\partial}{\partial y_i}\left(a_{ij}(\boldsymbol{y},t)\frac{\partial u^{(1)}}{\partial x_j}\right)\\
&-\frac{\partial}{\partial x_i}\left(a_{ij}(\boldsymbol{y},t)\left(\frac{\partial u^{(0)}}{\partial x_j}+\frac{\partial u^{(1)}}{\partial y_j}\right)\right)-f\\
&=(\rho(\boldsymbol{y},t)-\hat{\rho}(t))\frac{\partial^2 u^{(0)}}{\partial t^2}+(\mu(\boldsymbol{y},t)-\hat{\mu}(t))\frac{\partial u^{(0)}}{\partial t}\\
&+\left[\hat{a}_{ij}(t)-a_{ij}(\boldsymbol{y},t)-a_{im}(\boldsymbol{y},t)\frac{\partial N^j(\boldsymbol{y},t)}{\partial y_m}\right.\\
&\left.-\frac{\partial}{\partial y_m}(a_{mj}(\boldsymbol{y},t)N^i(\boldsymbol{y},t))\right]\frac{\partial^2 u^{(0)}}{\partial x_i\partial x_j}. \quad (10)
\end{aligned}$$

Thus $u^{(2)}$ can be defined as follows:

$$u^{(2)} = N^{\alpha_1\alpha_2}(\boldsymbol{y},t)\frac{\partial^2 u^{(0)}}{\partial x_{\alpha_1}\partial x_{\alpha_2}} + F(\boldsymbol{y},t)\frac{\partial^2 u^{(0)}}{\partial t^2} + G(\boldsymbol{y},t)\frac{\partial u^{(0)}}{\partial t}, \tag{11}$$

where $N^{\alpha_1\alpha_2}(\boldsymbol{y},t)$, $F(\boldsymbol{y},t)$, and $G(\boldsymbol{y},t)$ are the second-order auxiliary cell functions defined in unit cell Y. Substituting Eq. (11) into Eq. (10), we obtain a series of equations which attach the zero boundary condition

$$\begin{cases} \dfrac{\partial}{\partial y_i}\left(a_{ij}(\boldsymbol{y},t)\dfrac{\partial N^{\alpha_1\alpha_2}(\boldsymbol{y},t)}{\partial y_j}\right) \\ = \hat{a}_{\alpha_1\alpha_2}(t) - a_{\alpha_1\alpha_2}(\boldsymbol{y},t) - a_{\alpha_1 j}(\boldsymbol{y},t)\dfrac{\partial N^{\alpha_2}(\boldsymbol{y},t)}{\partial y_j}, \\ -\dfrac{\partial}{\partial y_i}(a_{i\alpha_1}(\boldsymbol{y},t)N^{\alpha_2}(\boldsymbol{y},t)), \quad (\boldsymbol{y},t)\in Y\times(0,T), \\ N^{\alpha_1\alpha_2}(\boldsymbol{y},t) = 0, \quad (\boldsymbol{y},t)\in \partial Y\times(0,T), \end{cases} \tag{12}$$

$$\begin{cases} \dfrac{\partial}{\partial y_i}\left(a_{ij}(\boldsymbol{y},t)\dfrac{\partial F(\boldsymbol{y},t)}{\partial y_j}\right) \\ = \rho(\boldsymbol{y},t) - \hat{\rho}(t), \quad (\boldsymbol{y},t)\in Y\times(0,T), \\ F(\boldsymbol{y},t) = 0, \quad (\boldsymbol{y},t)\in \partial Y\times(0,T), \end{cases} \tag{13}$$

$$\begin{cases} \dfrac{\partial}{\partial y_i}\left(a_{ij}(\boldsymbol{y},t)\dfrac{\partial G(\boldsymbol{y},t)}{\partial y_j}\right) \\ = \mu(\boldsymbol{y},t) - \hat{\mu}(t), \quad (\boldsymbol{y},t)\in Y\times(0,T), \\ G(\boldsymbol{y}) = 0, \quad (\boldsymbol{y},t)\in \partial Y\times(0,T). \end{cases} \tag{14}$$

Remark 3 According to the Lax–Milgram theorem and assumptions (A) and (B), it is easy to prove that problems (12)–(14) have a unique solution for any fixed time variable t.

Summing up, we define the FOTS and SOTS of problem (1) as follows:

$$u^{(1\varepsilon)} = u^{(0)} + \varepsilon N^{\alpha_1}(\boldsymbol{y},t)\frac{\partial u^{(0)}}{\partial x_{\alpha_1}}, \tag{15}$$

$$u^{(2\varepsilon)} = u^{(0)} + \varepsilon N^{\alpha_1}(\boldsymbol{y},t)\frac{\partial u^{(0)}}{\partial x_{\alpha_1}} + \varepsilon^2 N^{\alpha_1\alpha_2}(\boldsymbol{y},t)\frac{\partial^2 u^{(0)}}{\partial x_{\alpha_1}\partial x_{\alpha_2}} + \varepsilon^2 F(\boldsymbol{y},t)\frac{\partial^2 u^{(0)}}{\partial t^2} + \varepsilon^2 G(\boldsymbol{y},t)\frac{\partial u^{(0)}}{\partial t}. \tag{16}$$

Notably, the difference from the wave equation in Ref. [7] lies in that there exist second-order auxiliary cell functions $F(\boldsymbol{y},t)$ and $G(\boldsymbol{y},t)$ which are used to eliminate the effects of the inertial term and the damping term.

Theorem 1 The hyperbolic–parabolic equations (1) with rapidly oscillating coefficients have an SOTS approximate solution as follows:

$$\begin{aligned} & u^{(2\varepsilon)}(\boldsymbol{x},t) \\ &= u^{(0)}(\boldsymbol{x},t) + \varepsilon N^{\alpha_1}(\boldsymbol{y},t)\frac{\partial u^{(0)}(\boldsymbol{x},t)}{\partial x_{\alpha_1}} \\ &\quad + \varepsilon^2 N^{\alpha_1\alpha_2}(\boldsymbol{y},t)\frac{\partial^2 u^{(0)}(\boldsymbol{x},t)}{\partial x_{\alpha_1}\partial x_{\alpha_2}} + \varepsilon^2 F(\boldsymbol{y})\frac{\partial^2 u^{(0)}(\boldsymbol{x},t)}{\partial t^2} \\ &\quad + \varepsilon^2 G(\boldsymbol{y},t)\frac{\partial u^{(0)}(\boldsymbol{x},t)}{\partial t}, \end{aligned} \tag{17}$$

where $u^{(0)}$ is the solution of the homogenized problem (9), N^{α_1} is the first-order auxiliary cell function defined by Eq. (7), and $N^{\alpha_1\alpha_2}$, F, and G are the second-order auxiliary cell functions defined by Eqs. (12)–(14), respectively.

2.2. Error analysis in pointwise sense

In this subsection, we give the specific error analysis of FOTS and SOTS in the pointwise sense. Firstly, we denote the error functions of FOTS and SOTS as $\omega^{(1)}(\boldsymbol{x},t) = u^{(\varepsilon)}(\boldsymbol{x},t) - u^{(1\varepsilon)}(\boldsymbol{x},t)$ and $\omega^{(2)}(\boldsymbol{x},t) = u^{(\varepsilon)}(\boldsymbol{x},t) - u^{(2\varepsilon)}(\boldsymbol{x},t)$. Suppose that Ω is the union of the entire periodic cells, i.e., $\bar{\Omega} = \cup_{z\in T_\varepsilon}\varepsilon(z+Y)$, where the index set $T_\varepsilon = \{z\in\mathbb{Z}^n, \varepsilon(z+Y)\in\hat{\Omega}\}$. Let $E_z = \varepsilon(z+Y)$ and ∂E_z be the boundary of E_z. After a simple computation by substituting $\omega^{(1)}(\boldsymbol{x},t)$ for $u^{(\varepsilon)}(\boldsymbol{x},t)$ in problem (1), we obtain the following residual equations of FOTS for $(\boldsymbol{x},t)\in\Omega\times(0,T)$ which holds in the distribution sense:

$$\begin{cases} \rho^\varepsilon(\boldsymbol{x},t)\dfrac{\partial^2\omega^{(1)}(\boldsymbol{x},t)}{\partial t^2} + \mu^\varepsilon(\boldsymbol{x},t)\dfrac{\partial\omega^{(1)}(\boldsymbol{x},t)}{\partial t} \\ \quad - \dfrac{\partial}{\partial x_i}\left(a^\varepsilon_{ij}(\boldsymbol{x},t)\dfrac{\omega^{(1)}(\boldsymbol{x},t)}{\partial x_j}\right) \\ = f_0(\boldsymbol{x},\boldsymbol{y},t) + \varepsilon f_1(\boldsymbol{x},\boldsymbol{y},t), \quad (\boldsymbol{x},t)\in\Omega\times(0,T), \\ \omega^{(1)}(\boldsymbol{x},t) = 0, \quad (\boldsymbol{x},t)\in\partial\Omega\times(0,T), \\ \omega^{(1)}(\boldsymbol{x},0) = -\varepsilon N^{\alpha_1}(\boldsymbol{y},0)\dfrac{\partial u^{(0)}(\boldsymbol{x},0)}{\partial x_{\alpha_1}} = \varepsilon\psi_1(\boldsymbol{x}), \\ \dfrac{\partial\omega^{(1)}(\boldsymbol{x},t)}{\partial t}\Big|_{t=0} = -\varepsilon\dfrac{\partial}{\partial t}\left(N^{\alpha_1}(\boldsymbol{y},t)\dfrac{\partial u^0(\boldsymbol{x},t)}{\partial x_{\alpha_1}}\right)\Big|_{t=0} \\ \qquad = \varepsilon\psi_2(\boldsymbol{x}), \quad \boldsymbol{x}\in\Omega, \end{cases} \tag{18}$$

where

$$\begin{aligned} f_0(\boldsymbol{x},\boldsymbol{y},t) &= (\hat{\rho}(t) - \rho(\boldsymbol{y},t))\frac{\partial^2 u^{(0)}}{\partial t^2} + (\hat{\mu}(t) - \mu(\boldsymbol{y},t))\frac{\partial u^{(0)}}{\partial t} \\ &\quad - \left[\hat{a}_{ij}(t) - a_{ij}(\boldsymbol{y},t) - a_{ik}(\boldsymbol{y},t)\frac{\partial N^j(\boldsymbol{y},t)}{\partial y_k}\right. \\ &\quad \left. - \frac{\partial}{\partial y_k}(a_{kj}(\boldsymbol{y},t)N^i(\boldsymbol{y},t))\right]\frac{\partial^2 u^{(0)}}{\partial x_i\partial x_j}, \\ f_1(\boldsymbol{x},\boldsymbol{y},t) &= -\rho(\boldsymbol{y},t)N^{\alpha_1}(\boldsymbol{y},t)\frac{\partial^3 u^{(0)}}{\partial x_{\alpha_1}\partial t^2} \\ &\quad - \mu(\boldsymbol{y},t)N^{\alpha_1}(\boldsymbol{y},t)\frac{\partial^2 u^{(0)}}{\partial x_{\alpha_1}\partial t} \\ &\quad + a_{ij}(\boldsymbol{y},t)N^{\alpha_1}(\boldsymbol{y},t)\frac{\partial^3 u^{(0)}}{\partial x_{\alpha_1}\partial x_i\partial x_j}. \end{aligned} \tag{19}$$

Secondly, using the same method, we derive the following residual equation of SOTS which holds similarly in the

distribution sense:

$$\begin{cases}
\rho^{\varepsilon}(\boldsymbol{x},t)\dfrac{\partial^2\omega^{(2)}(\boldsymbol{x},t)}{\partial t^2}+\mu^{\varepsilon}(\boldsymbol{x},t)\dfrac{\partial\omega^{(2)}(\boldsymbol{x},t)}{\partial t}\\
-\dfrac{\partial}{\partial x_i}\left(a_{ij}^{\varepsilon}(\boldsymbol{x},t)\dfrac{\omega^{(2)}(\boldsymbol{x},t)}{\partial x_j}\right)\\
=\varepsilon\tilde{f}_1(\boldsymbol{x},\boldsymbol{y},t),\quad (\boldsymbol{x},t)\in\Omega\times(0,T),\\
\omega^{(2)}(\boldsymbol{x},t)=0,\quad (\boldsymbol{x},t)\in\partial\Omega\times(0,T),\\
\omega^{(2)}(\boldsymbol{x},0)=-\varepsilon N^{\alpha_1}(\boldsymbol{y},0)\dfrac{\partial u^{(0)}(\boldsymbol{x},0)}{\partial x_{\alpha_1}}\\
-\varepsilon^2 N^{\alpha_1\alpha_2}(\boldsymbol{y},0)\dfrac{\partial^2 u^{(0)}(\boldsymbol{x},0)}{\partial x_{\alpha_1}\partial x_{\alpha_2}}\\
-\varepsilon^2 F(\boldsymbol{y},0)\dfrac{\partial^2 u^{(0)}(\boldsymbol{x},t)}{\partial t^2}\Big|_{t=0},\\
-\varepsilon^2 G(\boldsymbol{y},0)\dfrac{\partial u^{(0)}(\boldsymbol{x},t)}{\partial t}\Big|_{t=0}=\varepsilon\tilde{\psi}_1(\boldsymbol{x}),\\
\dfrac{\partial\omega^{(2)}(\boldsymbol{x},t)}{\partial t}\Big|_{t=0}=-\varepsilon\dfrac{\partial}{\partial t}\left(N^{\alpha_1}(\boldsymbol{y},t)\dfrac{\partial u^{(0)}(\boldsymbol{x},t)}{\partial x_{\alpha_1}}\right)\Big|_{t=0}\\
-\varepsilon^2\dfrac{\partial}{\partial t}\left(N^{\alpha_1\alpha_2}(\boldsymbol{y},t)\dfrac{\partial^2 u^{(0)}(\boldsymbol{x},t)}{\partial x_{\alpha_1}\partial x_{\alpha_2}}\right)\Big|_{t=0}\\
-\varepsilon^2\dfrac{\partial}{\partial t}\left(F(\boldsymbol{y},t)\dfrac{\partial^2 u^{(0)}(\boldsymbol{x},t)}{\partial t^2}\right)\Big|_{t=0},\\
-\varepsilon^2\dfrac{\partial}{\partial t}\left(G(\boldsymbol{y},t)\dfrac{\partial u^{(0)}(\boldsymbol{x},t)}{\partial t}\right)\Big|_{t=0}=\varepsilon\tilde{\psi}_2(\boldsymbol{x}),\quad \boldsymbol{x}\in\Omega,
\end{cases}\tag{20}$$

where

$$\begin{aligned}
&\tilde{f}_1(\boldsymbol{x},\boldsymbol{y},t)\\
=&-\rho(\boldsymbol{y},t)N^{\alpha_1}(\boldsymbol{y},t)\frac{\partial^3 u^{(0)}}{\partial x_{\alpha_1}\partial t^2}-\varepsilon\rho(\boldsymbol{y},t)N^{\alpha_1\alpha_2}(\boldsymbol{y},t)\\
&\times\frac{\partial^4 u^{(0)}}{\partial x_{\alpha_1}\partial x_{\alpha_2}\partial t^2}-\varepsilon\rho(\boldsymbol{y},t)F(\boldsymbol{y},t)\frac{\partial^4 u^{(0)}}{\partial t^4}\\
&-\varepsilon\rho(\boldsymbol{y},t)G(\boldsymbol{y},t)\frac{\partial^3 u^{(0)}}{\partial t^3}-\mu(\boldsymbol{y},t)N^{\alpha_1}(\boldsymbol{y},t)\frac{\partial^2 u^{(0)}}{\partial x_{\alpha_1}\partial t}\\
&-\varepsilon\mu(\boldsymbol{y},t)N^{\alpha_1\alpha_2}(\boldsymbol{y},t)\frac{\partial^3 u^{(0)}}{\partial x_{\alpha_1}\partial x_{\alpha_2}\partial t}\\
&-\varepsilon\mu(\boldsymbol{y},t)F(\boldsymbol{y},t)\frac{\partial^3 u^{(0)}}{\partial t^3}-\varepsilon\mu(\boldsymbol{y},t)G(\boldsymbol{y},t)\frac{\partial^2 u^{(0)}}{\partial t^2}\\
&+a_{ij}(\boldsymbol{y},t)N^{\alpha_1}(\boldsymbol{y},t)\frac{\partial^3 u^{(0)}}{\partial x_{\alpha_1}\partial x_i\partial x_j}\\
&+a_{ij}(\boldsymbol{y},t)\frac{\partial N^{\alpha_1\alpha_2}(\boldsymbol{y},t)}{\partial y_j}\frac{\partial^3 u^{(0)}}{\partial x_{\alpha_1}\partial x_i\partial x_j}\\
&+\frac{\partial(a_{ij}(\boldsymbol{y},t)N^{\alpha_1\alpha_2}(\boldsymbol{y},t))}{\partial y_i}\frac{\partial^3 u^{(0)}}{\partial x_{\alpha_1}\partial x_i\partial x_j}\\
&+\varepsilon a_{ij}(\boldsymbol{y},t)N^{\alpha_1\alpha_2}(\boldsymbol{y},t)\frac{\partial^4 u^{(0)}}{\partial x_{\alpha_1}\partial x_{\alpha_2}\partial x_i\partial x_j}\\
&+a_{ij}(\boldsymbol{y},t)\frac{\partial F(\boldsymbol{y},t)}{\partial y_j}\frac{\partial^3 u^{(0)}}{\partial x_i\partial t^2}+\frac{\partial(a_{ij}(\boldsymbol{y})F(\boldsymbol{y},t))}{\partial y_j}\frac{\partial^3 u^{(0)}}{\partial x_j\partial t^2}\\
&+\varepsilon a_{ij}(\boldsymbol{y},t)F(\boldsymbol{y},t)\frac{\partial^4 u^{(0)}}{\partial x_i\partial x_j\partial t^2}+a_{ij}(\boldsymbol{y},t)\frac{\partial G(\boldsymbol{y},t)}{\partial y_j}\frac{\partial^2 u^{(0)}}{\partial x_i\partial t}\\
&+\frac{\partial(a_{ij}(\boldsymbol{y},t)G(\boldsymbol{y},t))}{\partial y_j}\frac{\partial^2 u^{(0)}}{\partial x_j\partial t}+\varepsilon a_{ij}(\boldsymbol{y},t)G(\boldsymbol{y},t)\frac{\partial^3 u^{(0)}}{\partial x_i\partial x_j\partial t}.
\end{aligned}\tag{21}$$

Now we can give a conclusion about the error analysis in the pointwise sense. From the residual equation (17), one easily finds that the residual of FOTS is O(1) in the pointwise sense due to the term $f_0(\boldsymbol{x},\boldsymbol{y},t)$. This is not acceptable in practical engineering calculation. However, it is easy to see from the residual equation (18) that the residual of SOTS is $O(\varepsilon)$ in the pointwise sense. Thus, the SOTS can have the required accuracy for engineering calculations and capture the the micro-scale behavior of composite materials when ε is a sufficiently small constant. This is the main reason and motivation to develop the SOTS.

3. Main convergence theorem and its proof

In this section, we give the proof of the explicit convergence order of SOTS in the integral sense for the hyperbolic–parabolic equations with rapidly oscillating coefficients. Moreover, we give the degradation of the hyperbolic–parabolic equation's error estimate. In order to obtain the explicit convergence order of SOTS, we need to give some lemmas first.

3.1. The regularity of auxiliary cell functions

As we all know, the auxiliary cell functions are defined with the periodic boundary conditions in the classical homogenization methods (see Refs. [22]–[24]). In this case, the auxiliary cell functions have enough regularity on the boundary of the unit cell. However, the normal derivatives of the auxiliary cell functions defined with the Dirichlet boundary conditions only are continuous on the boundary of the unit cell under the geometric symmetry and regularity assumptions of the hyperbolic–parabolic equation's coefficients (see Refs. [4]–[10]).

To obtain the regularity of the cell functions, we make the following assumptions similar to Refs. [6]–[10]:

(i) $a_{ij}^{\varepsilon}(\boldsymbol{x},t)\in C^1(\bar{\Omega}\times[0,T])$; $\rho^{\varepsilon}(\boldsymbol{x},t)\in C^0(\bar{\Omega}\times[0,T])$ $\mu^{\varepsilon}(\boldsymbol{x},t)\in C^0(\bar{\Omega}\times[0,T])$;

(ii) let $\Delta_1,\ldots,\Delta_n$ $(n=2,3)$ be the middle superplanes of the reference cell $Y=(0,1)^n$, then set $\boldsymbol{y}=\boldsymbol{x}/\varepsilon$ and assume that $a_{ii}(\boldsymbol{y},t),\rho(\boldsymbol{y},t),\mu(\boldsymbol{y},t)$ are symmetric with respect to $\Delta_1,\ldots,\Delta_n$ $(n=2,3)$ and $a_{ij}(\boldsymbol{y},t)$, $i\neq j$ are anti-symmetric with respect to $\Delta_1,\ldots,\Delta_n$ $(n=2,3)$ in Y for any fixed $t\in[0,T]$.

Lemma 1 Under assumptions (A)–(C) and (i) and (ii), the normal derivatives $\sigma_Y(N^{\alpha_1})$, $\sigma_Y(N^{\alpha_1\alpha_2})$, $\sigma_Y(F)$, and $\sigma_Y(G)$ can be proved to be continuous on the boundary for any fixed $t\in[0,T]$ by using the same method in Refs. [6]–[10], where operator $\sigma_Y=n_i a_{ij}^{\varepsilon}(\boldsymbol{x},t)\frac{\partial}{\partial x_j}$.

3.2. The proof of convergence theorem

Theorem 2 Suppose that $\Omega \subset \mathbb{R}^n$ is the union of the entire periodic cells, i.e., $\bar{\Omega} = \cup_{z\in T_\varepsilon} \varepsilon(z+Y)$, where the index set $T_\varepsilon = \{z \in Z^n, \varepsilon(z+Y) \subset \hat{\Omega}\}$. Let $u^\varepsilon(\boldsymbol{x},t)$ and $u^{(0)}(\boldsymbol{x},t)$ be the weak solutions of problem (1) and the associated homogenized problem (9). The second-order two-scale solution is defined in Theorem 1. Under assumptions (A)–(C) and (i) and (ii), if $\partial a_{ij}^\varepsilon/\partial t \in L^\infty(\Omega\times[0,T])$, $u^{(0)} \in L^2(0,T;H^4(\Omega))$, $\partial u^{(0)}/\partial t \in L^2(0,T;H^2(\Omega))$, $\partial^2 u^{(0)}/(\partial t^2) \in L^2(0,T;H^2(\Omega))$; then we have the following error estimate of SOTS for the hyperbolic–parabolic equations with rapidly oscillating coefficients:

$$\left\| \frac{\partial \omega^{(2)}(\boldsymbol{x},t)}{\partial t} \right\|_{L^\infty(0,T;L^2(\Omega))} + \left\| \omega^{(2)}(\boldsymbol{x},t) \right\|_{L^\infty(0,T;H_0^1(\Omega))} \le C(T)\varepsilon, \tag{22}$$

where $C(T)$ is a constant independent of ε, but dependent on T.

Proof Firstly, from Eqs. (7), (8), and (12)–(14), we have the following result:

$$\begin{aligned}
&\sigma_Y(u^{(2\varepsilon)}) \\
&= n_i a_{ij}^\varepsilon(\boldsymbol{x},t)\frac{\partial u^{(2\varepsilon)}}{\partial x_j} \\
&= n_i a_{ij}(\boldsymbol{y},t)\left(\frac{\partial u^{(2\varepsilon)}}{\partial x_j} + \frac{1}{\varepsilon}\frac{\partial u^{(2\varepsilon)}}{\partial y_j}\right) \\
&= n_i a_{ij}(\boldsymbol{y},t)\left(\frac{\partial}{\partial x_j} + \frac{1}{\varepsilon}\frac{\partial}{\partial y_j}\right) \\
&\quad \times \left(u^{(0)} + \varepsilon N^{\alpha_1}(\boldsymbol{y},t)\frac{\partial u^{(0)}}{\partial x_{\alpha_1}} + \varepsilon^2 N^{\alpha_1\alpha_2}(\boldsymbol{y},t)\frac{\partial^2 u^{(0)}}{\partial x_{\alpha_1}\partial x_{\alpha_2}}\right. \\
&\quad \left. + \varepsilon^2 F(\boldsymbol{y},t)\frac{\partial^2 u^{(0)}}{\partial t^2} + \varepsilon^2 G(\boldsymbol{y},t)\frac{\partial u^{(0)}}{\partial t}\right) \\
&= n_i a_{ij}(\boldsymbol{y},t)\left(\frac{\partial u^{(0)}}{\partial x_j} + \varepsilon N^{\alpha_1}(\boldsymbol{y},t)\frac{\partial^2 u^{(0)}}{\partial x_{\alpha_1}\partial x_j}\right. \\
&\quad + \varepsilon^2 N^{\alpha_1\alpha_2}(\boldsymbol{y},t)\frac{\partial^3 u^{(0)}}{\partial x_{\alpha_1}\partial x_{\alpha_2}\partial x_j} \\
&\quad \left. + \varepsilon^2 F(\boldsymbol{y},t)\frac{\partial^3 u^{(0)}}{\partial t^2\partial x_j} + \varepsilon^2 G(\boldsymbol{y},t)\frac{\partial^2 u^{(0)}}{\partial t\partial x_j}\right) \\
&\quad + \left(\sigma_Y(N^{\alpha_1}(\boldsymbol{y},t))\frac{\partial u^{(0)}}{\partial x_{\alpha_1}} + \varepsilon\sigma_Y(N^{\alpha_1\alpha_2}(\boldsymbol{y},t))\frac{\partial^2 u^{(0)}}{\partial x_{\alpha_1}\partial x_{\alpha_2}}\right. \\
&\quad \left. + \varepsilon\sigma_Y(F(\boldsymbol{y},t))\frac{\partial^2 u^{(0)}}{\partial t^2} + \varepsilon\sigma_Y(G(\boldsymbol{y},t))\frac{\partial u^{(0)}}{\partial t}\right).
\end{aligned} \tag{23}$$

This formula will be used in the following proof.

Secondly, we use the residual equation (18) to complete the error estimate of SOTS for the hyperbolic–parabolic equations with rapidly oscillating coefficients. Since $\partial\omega^{(2)}/\partial t$ is in $L^\infty(0,T;L^2(\Omega))$, we cannot use $\partial\omega^{(2)}/\partial t$ as the test function for residual equation (18) directly. To overcome this difficulty, we use the density argument (see Refs. [6], [7], and [24]). In order to simplify the process of proof, we omit this detail. Then, multiplying $\partial\omega^{(2)}/\partial t$ on both sides of Eq. (18) and integrating by parts on Ω, we obtain

$$\begin{aligned}
&\int_\Omega \left[\rho^\varepsilon \frac{\partial^2\omega^{(2)}}{\partial t^2} + \mu^\varepsilon \frac{\partial\omega^{(2)}}{\partial t} - \frac{\partial}{\partial x_i}\left(a_{ij}^\varepsilon \frac{\partial\omega^{(2)}}{\partial x_j}\right)\right]\frac{\partial\omega^{(2)}}{\partial t}\,\mathrm{d}\Omega \\
&= \int_\Omega \varepsilon\tilde{f}_1 \frac{\partial\omega^{(2)}}{\partial t}\,\mathrm{d}\Omega.
\end{aligned} \tag{24}$$

Using Green's formula to simplify the above identity (21), we obtain

$$\begin{aligned}
&\int_\Omega \rho^\varepsilon \frac{\partial^2\omega^{(2)}}{\partial t^2}\frac{\partial\omega^{(2)}}{\partial t}\,\mathrm{d}\Omega + \int_\Omega \mu^\varepsilon \frac{\partial\omega^{(2)}}{\partial t}\frac{\partial\omega^{(2)}}{\partial t}\,\mathrm{d}\Omega \\
&+ \int_\Omega a_{ij}^\varepsilon \frac{\partial\omega^{(2)}}{\partial x_j}\frac{\partial}{\partial x_i}\left(\frac{\partial\omega^{(2)}}{\partial t}\right)\mathrm{d}\Omega \\
&= \int_\Omega \varepsilon\tilde{f}_1\frac{\partial\omega^{(2)}}{\partial t}\,\mathrm{d}\Omega + \int_{\cup_{z\in T_\varepsilon}\partial E_z} r_2 \frac{\partial\omega^{(2)}}{\partial t}\,\mathrm{d}\Gamma_{\boldsymbol{y}},
\end{aligned} \tag{25}$$

where r_2 results from using the Green's formula on ∂E_z (see Refs. [25] and [26]).

Combining Eq. (20) and Lemma 2, we obtain

$$\begin{aligned}
\left\langle r_2, \frac{\partial\omega^{(2)}}{\partial t}\right\rangle &= \sum_{z\in T_\varepsilon}\int_{\partial E_z} \sigma_Y(u^\varepsilon - u^{(2\varepsilon)})\frac{\partial\omega^{(2)}}{\partial t}\,\mathrm{d}\Gamma_{\boldsymbol{y}} \\
&= -\sum_{z\in T_\varepsilon}\int_{\partial E_z}\sigma_Y(u^{(2\varepsilon)})\frac{\partial\omega^{(2)}}{\partial t}\,\mathrm{d}\Gamma_{\boldsymbol{y}} = 0.
\end{aligned} \tag{26}$$

After that, we can easily derive the following identity by combining Eqs. (22) and (23):

$$\begin{aligned}
&\frac{1}{2}\frac{\partial}{\partial t}\left[\int_\Omega \rho^\varepsilon\left(\frac{\partial\omega^{(2)}}{\partial t}\right)^2\mathrm{d}\Omega + \int_\Omega a_{ij}^\varepsilon\frac{\partial\omega^{(2)}}{\partial x_j}\frac{\partial\omega^{(2)}}{\partial x_i}\,\mathrm{d}\Omega\right] \\
&- \frac{1}{2}\int_\Omega \frac{\partial a_{ij}^\varepsilon}{\partial t}\frac{\partial\omega^{(2)}}{\partial x_j}\frac{\partial\omega^{(2)}}{\partial x_i}\,\mathrm{d}\Omega \\
&+ \int_\Omega \mu^\varepsilon\frac{\partial\omega^{(2)}}{\partial t}\frac{\partial\omega^{(2)}}{\partial t}\,\mathrm{d}\Omega = \int_\Omega \varepsilon\tilde{f}_1\frac{\partial\omega^{(2)}}{\partial t}\,\mathrm{d}\Omega.
\end{aligned} \tag{27}$$

Then, we integrate both sides from 0 to t $(0 < t \le T)$ and obtain

$$\begin{aligned}
&\int_0^t \frac{\partial}{\partial\tau}\left[\int_\Omega \rho^\varepsilon\left(\frac{\partial\omega^{(2)}}{\partial t}\right)^2\mathrm{d}\Omega\right]\mathrm{d}\tau \\
&+ \int_0^t \frac{\partial}{\partial\tau}\left[\int_\Omega a_{ij}^\varepsilon\frac{\partial\omega^{(2)}}{\partial x_j}\frac{\partial\omega^{(2)}}{\partial x_i}\,\mathrm{d}\Omega\right]\mathrm{d}\tau \\
&- \int_0^t\int_\Omega \frac{\partial a_{ij}^\varepsilon}{\partial\tau}\frac{\partial\omega^{(2)}}{\partial x_j}\frac{\partial\omega^{(2)}}{\partial x_i}\,\mathrm{d}\Omega\,\mathrm{d}\tau \\
&+ 2\int_0^t\int_\Omega \mu^\varepsilon\frac{\partial\omega^{(2)}}{\partial\tau}\frac{\partial\omega^{(2)}}{\partial\tau}\,\mathrm{d}\Omega\,\mathrm{d}\tau \\
&= 2\int_0^t\int_\Omega \varepsilon\tilde{f}_1\frac{\partial\omega^{(2)}}{\partial\tau}\,\mathrm{d}\Omega\,\mathrm{d}\tau.
\end{aligned} \tag{28}$$

After a simple calculation, we obtain the following equation:

$$\int_\Omega \rho^\varepsilon(\boldsymbol{x},t)\left(\frac{\partial\omega^{(2)}(\boldsymbol{x},t)}{\partial t}\right)^2\mathrm{d}\Omega$$

$$
\begin{aligned}
&+\int_\Omega a_{ij}^\varepsilon(\boldsymbol{x},t)\frac{\partial\omega^{(2)}(\boldsymbol{x},t)}{\partial x_j}\frac{\partial\omega^{(2)}(\boldsymbol{x},t)}{\partial x_i}\,\mathrm{d}\Omega\\
&+2\int_0^t\int_\Omega \mu^\varepsilon(\boldsymbol{x},\tau)\frac{\partial\omega^{(2)}(\boldsymbol{x},\tau)}{\partial\tau}\frac{\partial\omega^{(2)}(\boldsymbol{x},\tau)}{\partial\tau}\,\mathrm{d}\Omega\,\mathrm{d}\tau\\
=&\int_\Omega \rho^\varepsilon(\boldsymbol{x},0)\left(\frac{\partial\omega^{(2)}(\boldsymbol{x},t)}{\partial t}\bigg|_{t=0}\right)^2\mathrm{d}\Omega\\
&+\int_\Omega a_{ij}^\varepsilon(\boldsymbol{x},0)\frac{\partial\omega^{(2)}(\boldsymbol{x},0)}{\partial x_j}\frac{\partial\omega^{(2)}(\boldsymbol{x},0)}{\partial x_i}\,\mathrm{d}\Omega\\
&+\int_0^t\int_\Omega \frac{\partial a_{ij}^\varepsilon(\boldsymbol{x},\tau)}{\partial\tau}\frac{\partial\omega^{(2)}(\boldsymbol{x},\tau)}{\partial x_j}\frac{\partial\omega^{(2)}(\boldsymbol{x},\tau)}{\partial x_i}\,\mathrm{d}\Omega\,\mathrm{d}\tau\\
&+2\int_0^t\int_\Omega \varepsilon\tilde{f}_1\frac{\partial\omega^{(2)}(\boldsymbol{x},\tau)}{\partial\tau}\,\mathrm{d}\Omega\,\mathrm{d}\tau. \qquad (29)
\end{aligned}
$$

Then substituting the initial conditions and the boundary conditions of residual equation (18) into the above identity (26), we have

$$
\begin{aligned}
&\int_\Omega \rho^\varepsilon(\boldsymbol{x},t)\left(\frac{\partial\omega^{(2)}(\boldsymbol{x},t)}{\partial t}\right)^2\mathrm{d}\Omega\\
&+\int_\Omega a_{ij}^\varepsilon(\boldsymbol{x},t)\frac{\partial\omega^{(2)}(\boldsymbol{x},t)}{\partial x_j}\frac{\partial\omega^{(2)}(\boldsymbol{x},t)}{\partial x_i}\,\mathrm{d}\Omega\\
&+2\int_0^t\int_\Omega \mu^\varepsilon(\boldsymbol{x},\tau)\frac{\partial\omega^{(2)}(\boldsymbol{x},\tau)}{\partial\tau}\frac{\partial\omega^{(2)}(\boldsymbol{x},\tau)}{\partial\tau}\,\mathrm{d}\Omega\,\mathrm{d}\tau\\
=&\int_\Omega \rho^\varepsilon(\boldsymbol{x},0)\,(\varepsilon\tilde{\psi}_2(\boldsymbol{x}))^2\,\mathrm{d}\Omega\\
&+\int_\Omega a_{ij}^\varepsilon(\boldsymbol{x},0)\frac{\partial(\varepsilon\tilde{\psi}_1(\boldsymbol{x}))}{\partial x_j}\frac{\partial(\varepsilon\tilde{\psi}_1(\boldsymbol{x}))}{\partial x_i}\,\mathrm{d}\Omega\\
&+\int_0^t\int_\Omega \frac{\partial a_{ij}^\varepsilon(\boldsymbol{x},\tau)}{\partial\tau}\frac{\partial\omega^{(2)}(\boldsymbol{x},\tau)}{\partial x_j}\frac{\partial\omega^{(2)}(\boldsymbol{x},\tau)}{\partial x_i}\,\mathrm{d}\Omega\,\mathrm{d}\tau\\
&+2\int_0^t\int_\Omega \varepsilon\tilde{f}_1\frac{\partial\omega^{(2)}(\boldsymbol{x},\tau)}{\partial\tau}\,\mathrm{d}\Omega\,\mathrm{d}\tau. \qquad (30)
\end{aligned}
$$

So far, we have obtained the essential identity for Theorem 3. Starting from here, we will give the final proof. First of all, owing to assumptions (A) and (B) and using the Poincaré–Friedrichs inequality, we have the following inequality by transforming the left side of Eq. (27):

$$
\begin{aligned}
&\int_\Omega \rho^\varepsilon(\boldsymbol{x},t)\left(\frac{\partial\omega^{(2)}(\boldsymbol{x},t)}{\partial t}\right)^2\mathrm{d}\Omega\\
&+\int_\Omega a_{ij}^\varepsilon(\boldsymbol{x},t)\frac{\partial\omega^{(2)}(\boldsymbol{x},t)}{\partial x_j}\frac{\partial\omega^{(2)}(\boldsymbol{x},t)}{\partial x_i}\,\mathrm{d}\Omega\\
&+2\int_0^t\int_\Omega \mu^\varepsilon(\boldsymbol{x},\tau)\frac{\partial\omega^{(2)}(\boldsymbol{x},\tau)}{\partial\tau}\frac{\partial\omega^{(2)}(\boldsymbol{x},\tau)}{\partial\tau}\,\mathrm{d}\Omega\,\mathrm{d}\tau\\
\geq&\left\|\sqrt{\rho^0}\frac{\partial\omega^{(2)}(\boldsymbol{x},t)}{\partial t}\right\|^2_{L^2(\Omega)}+C_1\left\|\omega^{(2)}(\boldsymbol{x},t)\right\|^2_{H_0^1(\Omega)}\\
&+2\mu^0\int_0^t\left\|\frac{\partial\omega^{(2)}(\boldsymbol{x},\tau)}{\partial\tau}\right\|^2_{L^2(\Omega)}\mathrm{d}\tau. \qquad (31)
\end{aligned}
$$

Then, due to $\partial a_{ij}^\varepsilon/\partial t\in L^\infty(\Omega\times[0,T])$ and Schwarz's inequality,

$$
\begin{aligned}
&\left|\int_0^t\int_\Omega \frac{\partial a_{ij}^\varepsilon(\boldsymbol{x},\tau)}{\partial\tau}\frac{\partial\omega^{(2)}(\boldsymbol{x},\tau)}{\partial x_j}\frac{\partial\omega^{(2)}(\boldsymbol{x},\tau)}{\partial x_i}\,\mathrm{d}\Omega\,\mathrm{d}\tau\right|\\
\leq&\left|\int_0^t\int_\Omega M_{ij}\frac{\partial\omega^{(2)}(\boldsymbol{x},\tau)}{\partial x_j}\frac{\partial\omega^{(2)}(\boldsymbol{x},\tau)}{\partial x_i}\,\mathrm{d}\Omega\,\mathrm{d}\tau\right|\\
\leq& M\int_0^t\left|\omega^{(2)}(\boldsymbol{x},\tau)\right|^2_{H_0^1(\Omega)}\mathrm{d}\tau\\
\leq& M\int_0^t\|\,\omega^{(2)}(\boldsymbol{x},\tau)\,\|^2_{H_0^1(\Omega)}\,\mathrm{d}\tau. \qquad (32)
\end{aligned}
$$

After that, using the Young's inequality $ab\leq(\lambda a^2+\lambda b^2/\lambda)/2,\forall\lambda\in\mathbb{R}^+$ with parameter λ and assumptions (A)–(C), and choosing the same parameter λ at $\forall\tau\in[0,t]$, we obtain the following inequality by transforming the right side of Eq. (27):

$$
\begin{aligned}
&\int_\Omega \rho^\varepsilon(\boldsymbol{x},0)\,(\varepsilon\tilde{\psi}_2(\boldsymbol{x}))^2\,\mathrm{d}\Omega\\
&+\int_\Omega a_{ij}^\varepsilon(\boldsymbol{x},0)\frac{\partial(\varepsilon\tilde{\psi}_1(\boldsymbol{x}))}{\partial x_j}\frac{\partial(\varepsilon\tilde{\psi}_1(\boldsymbol{x}))}{\partial x_i}\,\mathrm{d}\Omega\\
&+\int_0^t\int_\Omega \frac{\partial a_{ij}^\varepsilon(\boldsymbol{x},\tau)}{\partial\tau}\frac{\partial\omega^{(2)}(\boldsymbol{x},\tau)}{\partial x_j}\frac{\partial\omega^{(2)}(\boldsymbol{x},\tau)}{\partial x_i}\,\mathrm{d}\Omega\,\mathrm{d}\tau\\
&+2\int_0^t\int_\Omega \varepsilon\tilde{f}_1\frac{\partial\omega^{(2)}(\boldsymbol{x},\tau)}{\partial\tau}\,\mathrm{d}\Omega\,\mathrm{d}\tau\\
\leq&\int_\Omega \rho^\varepsilon(\boldsymbol{x},0)\,(\varepsilon\tilde{\psi}_2(\boldsymbol{x}))^2\,\mathrm{d}\Omega\\
&+\int_\Omega a_{ij}^\varepsilon(\boldsymbol{x},0)\frac{\partial(\varepsilon\tilde{\psi}_1(\boldsymbol{x}))}{\partial x_j}\frac{\partial(\varepsilon\tilde{\psi}_1(\boldsymbol{x}))}{\partial x_i}\,\mathrm{d}\Omega\\
&+M\int_0^t\|\,\omega^{(2)}(\boldsymbol{x},\tau)\,\|^2_{H_0^1(\Omega)}\,\mathrm{d}\tau\\
&+\frac{1}{\lambda}\int_0^t\left\|\varepsilon\tilde{f}_1\right\|^2_{L^2(\Omega)}\mathrm{d}\tau+\lambda\int_0^t\left\|\frac{\partial\omega^{(2)}(\boldsymbol{x},\tau)}{\partial\tau}\right\|^2_{L^2(\Omega)}\mathrm{d}\tau\\
\leq& C\varepsilon^2\|\tilde{\psi}_2(\boldsymbol{x})\|^2_{L^2(\Omega)}+\varepsilon^2\gamma_1\,|\tilde{\psi}_1(\boldsymbol{x})|^2_{H^1(\Omega)}\\
&+M\int_0^t\|\,\omega^{(2)}(\boldsymbol{x},\tau)\,\|^2_{H_0^1(\Omega)}\,\mathrm{d}\tau+\frac{1}{\lambda}\int_0^T\left\|\varepsilon\tilde{f}_1\right\|^2_{L^2(\Omega)}\mathrm{d}\tau\\
&+\lambda\int_0^t\left\|\frac{\partial\omega^{(2)}(\boldsymbol{x},\tau)}{\partial\tau}\right\|^2_{L^2(\Omega)}\mathrm{d}\tau\\
\leq& C(T)\varepsilon^2+M\int_0^t\|\,\omega^{(2)}(\boldsymbol{x},\tau)\,\|^2_{H_0^1(\Omega)}\,\mathrm{d}\tau\\
&+\lambda\int_0^t\left\|\frac{\partial\omega^{(2)}(\boldsymbol{x},\tau)}{\partial\tau}\right\|^2_{L^2(\Omega)}\mathrm{d}\tau. \qquad (33)
\end{aligned}
$$

Choosing a sufficiently big $\lambda>0$ fulfilled $\lambda-2\mu^0>0$ and combining Eqs. (28) and (30), we have

$$
\begin{aligned}
&\left\|\sqrt{\rho^0}\frac{\partial\omega^{(2)}(\boldsymbol{x},t)}{\partial t}\right\|^2_{L^2(\Omega)}+C_1\left\|\omega^{(2)}(\boldsymbol{x},t)\right\|^2_{H_0^1(\Omega)}\\
\leq& C(T)\varepsilon^2+M\int_0^t\|\,\omega^{(2)}(\boldsymbol{x},\tau)\,\|^2_{H_0^1(\Omega)}\,\mathrm{d}\tau\\
&+(\lambda-2\mu^0)\int_0^t\left\|\frac{\partial\omega^{(2)}(\boldsymbol{x},\tau)}{\partial\tau}\right\|^2_{L^2(\Omega)}\mathrm{d}\tau. \qquad (34)
\end{aligned}
$$

Denoting $\delta_1 = \min(\rho^0, C_1)$ and $\delta_2 = \max(M, \lambda - 2\mu^0)$, we have

$$\delta_1 \left(\left\| \frac{\partial \omega^{(2)}(\boldsymbol{x},t)}{\partial t} \right\|^2_{L^2(\Omega)} + \left\| \omega^{(2)}(\boldsymbol{x},t) \right\|^2_{H_0^1(\Omega)} \right) \le C(T)\varepsilon^2 + \delta_2 \left(\int_0^t \| \omega^{(2)}(\boldsymbol{x},\tau) \|^2_{H_0^1(\Omega)} \, \mathrm{d}\tau + \int_0^t \left\| \frac{\partial \omega^{(2)}(\boldsymbol{x},\tau)}{\partial \tau} \right\|^2_{L^2(\Omega)} \mathrm{d}\tau \right). \tag{35}$$

Without loss of generality, we denote $C(T) = C(T)/\delta_1$ and $\delta = \delta_2/\delta_1$ and obtain the following inequality:

$$\left\| \frac{\partial \omega^{(2)}(\boldsymbol{x},t)}{\partial t} \right\|^2_{L^2(\Omega)} + \left\| \omega^{(2)}(\boldsymbol{x},t) \right\|^2_{H_0^1(\Omega)} \le C(T)\varepsilon^2 + \delta \left(\int_0^t \| \omega^{(2)}(\boldsymbol{x},\tau) \|^2_{H_0^1(\Omega)} \, \mathrm{d}\tau + \int_0^t \left\| \frac{\partial \omega^{(2)}(\boldsymbol{x},\tau)}{\partial \tau} \right\|^2_{L^2(\Omega)} \mathrm{d}\tau \right). \tag{36}$$

Setting

$$\Theta(t) = \left\| \frac{\partial \omega^{(2)}(\boldsymbol{x},t)}{\partial t} \right\|^2_{L^2(\Omega)} + \left\| \omega^{(2)}(\boldsymbol{x},t) \right\|^2_{H_0^1(\Omega)},$$

then we obtain $\Theta(t) \le C(T)\varepsilon^2 + \delta \int_0^t \Theta(\tau)\mathrm{d}\tau$ from Eq. (33). It follows from Gronwall's inequality (see Ref. [24]) that $\Theta(t) \le C(T)\varepsilon^2$. consequently, we obtain the following result:

$$\left\| \frac{\partial \omega^{(2)}(\boldsymbol{x},t)}{\partial t} \right\|^2_{L^2(\Omega)} + \left\| \omega^{(2)}(\boldsymbol{x},t) \right\|^2_{H_0^1(\Omega)} \le C(T)\varepsilon^2, \quad \forall t \in [0,T]. \tag{37}$$

Then by using the AM–GM inequality $(a+b)/2 \le \sqrt{a^2+b^2/2}$ to the left side of inequality (34), the following equality is obtained:

$$2\left(\frac{\|\partial \omega^{(2)}(\boldsymbol{x},t)/\partial t\|_{L^2(\Omega)} + \|\omega^{(2)}(\boldsymbol{x},t)\|_{H_0^1(\Omega)}}{2} \right)^2 \le \left\| \frac{\partial \omega^{(2)}(\boldsymbol{x},t)}{\partial t} \right\|^2_{L^2(\Omega)} + \left\| \omega^{(2)}(\boldsymbol{x},t) \right\|^2_{H_0^1(\Omega)} \le C(T)\varepsilon^2, \quad \forall t \in [0,T]. \tag{38}$$

With the arbitrariness of time variable t and squaring root on both sides of inequality (35), we obtain the final convergence result

$$\left\| \frac{\partial \omega^{(2)}(\boldsymbol{x},t)}{\partial t} \right\|_{L^\infty(0,T;L^2(\Omega))} + \left\| \omega^{(2)}(\boldsymbol{x},t) \right\|_{L^\infty(0,T;H_0^1(\Omega))} \le C(T)\varepsilon, \tag{39}$$

where $C(T)$ is a constant independent of ε, but dependent on T.

3.3. The degradation of Theorem 2

In this section, we give the SOTS's convergence theorem of the hyperbolic equation by the degradation of Theorem 2. In general, for $\rho^\varepsilon \neq 0$ and $\mu^\varepsilon = 0$, equation (1) is called the hyperbolic wave equation, which describes the wave scattering and diffraction behavior of the composite structure. In the past, the convergence analysis of the hyperbolic equation is done separately. Now, we can obtain the convergence results of the hyperbolic equation from the degradation of Theorem 2.

Theorem 3 Assume that the definitions of $\Omega, \bar{\Omega}, T_\varepsilon, u^\varepsilon(\boldsymbol{x},t)$, $u^{(0)}(\boldsymbol{x},t)$ are the same as those in Theorem 2. It is easy to know that $\hat{\mu}(t) = 0$ and $G(\boldsymbol{y},t) = 0$ when $\rho^\varepsilon \neq 0$ and $\mu^\varepsilon = 0$. Under assumptions (A)–(C) and (i) and (ii), if $\partial a_{ij}^\varepsilon/\partial t \in L^\infty(\Omega \times [0,T])$, $u^{(0)} \in L^2(0,T;H^4(\Omega))$, $\partial u^{(0)}/\partial t \in L^2(0,T;H^2(\Omega))$, $\partial^2 u^{(0)}/\partial t^2 \in L^2(0,T;H^2(\Omega))$; then we have the following error estimate of SOTS for the hyperbolic wave equation with rapidly oscillating coefficients:

$$\left\| \frac{\partial \omega^{(2)}(\boldsymbol{x},t)}{\partial t} \right\|_{L^\infty(0,T;L^2(\Omega))} + \left\| \omega^{(2)}(\boldsymbol{x},t) \right\|_{L^\infty(0,T;H_0^1(\Omega))} \le C(T)\varepsilon, \tag{40}$$

where $C(T)$ is a constant independent of ε, but dependent on T.

Proof Under the situation of $\rho^\varepsilon \neq 0$ and $\mu^\varepsilon = 0$, the term $\int_\Omega \mu^\varepsilon \frac{\partial \omega^{(2)}}{\partial t} \frac{\partial \omega^{(2)}}{\partial t} \mathrm{d}\Omega$ in Eq. (22) is equal to 0. From the proof of Theorem 2, it is easy to know that the error estimate of SOTS for the hyperbolic wave equation still fulfils inequality (31)

$$\begin{aligned} &\left\| \sqrt{\rho^0} \frac{\partial \omega^{(2)}(\boldsymbol{x},t)}{\partial t} \right\|^2_{L^2(\Omega)} + C_1 \left\| \omega^{(2)}(\boldsymbol{x},t) \right\|^2_{H_0^1(\Omega)} \\ &\le C(T)\varepsilon^2 + M \int_0^t \| \omega^{(2)}(\boldsymbol{x},\tau) \|^2_{H_0^1(\Omega)} \, \mathrm{d}\tau + (\lambda - 2\mu^0) \int_0^t \left\| \frac{\partial \omega^{(2)}(\boldsymbol{x},\tau)}{\partial \tau} \right\|^2_{L^2(\Omega)} \mathrm{d}\tau \\ &= C(T)\varepsilon^2 + M \int_0^t \| \omega^{(2)}(\boldsymbol{x},\tau) \|^2_{H_0^1(\Omega)} \, \mathrm{d}\tau + \lambda \int_0^t \left\| \frac{\partial \omega^{(2)}(\boldsymbol{x},\tau)}{\partial \tau} \right\|^2_{L^2(\Omega)} \mathrm{d}\tau, \end{aligned} \tag{41}$$

where the constant $\mu^0 = 0$ due to $\mu^\varepsilon = 0$.

Then using the same proof method and denoting $\delta_1 = \min(\rho^0, C_1)$ and $\delta_2 = \lambda$, we can obtain the following inequality:

$$\delta_1 \left(\left\| \frac{\partial \omega^{(2)}(\boldsymbol{x},t)}{\partial t} \right\|^2_{L^2(\Omega)} + \left\| \omega^{(2)}(\boldsymbol{x},t) \right\|^2_{H_0^1(\Omega)} \right) \le C(T)\varepsilon^2 + \delta_2 \left(\int_0^t \| \omega^{(2)}(\boldsymbol{x},\tau) \|^2_{H_0^1(\Omega)} \, \mathrm{d}\tau + \int_0^t \left\| \frac{\partial \omega^{(2)}(\boldsymbol{x},\tau)}{\partial \tau} \right\|^2_{L^2(\Omega)} \mathrm{d}\tau \right). \tag{42}$$

After that, using Gronwall's inequality (see Ref. [6] and [7]) and AM–GM inequality $\frac{a+b}{2} \leq \sqrt{\frac{a^2+b^2}{2}}$ to inequality (42), and mimicking the proof process of Theorem 2, we obtain the final convergence result of the hyperbolic wave equation as follows:

$$\left\| \frac{\partial \omega^{(2)}(x,t)}{\partial t} \right\|_{L^\infty(0,T;L^2(\Omega))} + \left\| \omega^{(2)}(x,t) \right\|_{L^\infty(0,T;H_0^1(\Omega))} \leq C(T)\varepsilon. \tag{43}$$

The obtained convergence result of the hyperbolic wave equation is in completely accord with that in Ref. [7].

4. Second-order two-scale numerical method

In this section, we firstly give the finite element approximation schemes for the auxiliary cell problems and the homogenization problem of hyperbolic–parabolic equations (1). Then, we present a second-order two-scale numerical method to efficiently solve hyperbolic–parabolic equations (1).

4.1. Finite element approximation schemes of auxiliary cell problems and homogenization problem

It is easy to see that auxiliary cell problems (7) and (12)–(14) are all elliptic equations, where the time variable t only plays the role of a parameter. So we can solve these auxiliary cell problems with the standard finite element method. Considering the internal geometric structure complexity of the unit cell, we should use the triangular element in $\mathbb{R}^2$ and the tetrahedral element in $\mathbb{R}^3$ to solve the auxiliary cell problems. Without loss of generality, we only discuss the two-dimensional problem in this paper. Let $J^h = \{K\}$ be a regular family of triangulation of the reference unit cell Y, where $h = \max_K\{h_K\}$. Define the linear conforming finite element space for solving the auxiliary cell problems as $V_h = \{v \in C^0(Y) : v\,|_{\partial Y} = 0, v\,|_K \in P_1(K)\} \in H_0^1(Y)$.

As we all know, the homogenized coefficients $\hat{a}_{ij}(t)$ are derived from Eq. (8). So $\hat{a}_{ij}(t)$ depend on the finite element calculation of the auxiliary cell problem $N^{\alpha_1}(y,t)$. Suppose that $N_h^{\alpha_1}(x,y,t)$ are the corresponding finite element solutions of $N^{\alpha_1}(x,y,t)$. If we denote $\hat{a}_{ij}^h(t)$ as the finite element approximation of the homogenized coefficients $\hat{a}_{ij}(t)$, then $\hat{a}_{ij}^h(t)$ will be calculated by the formula

$$\hat{a}_{ij}^h(t) = \frac{1}{|Y|}\int_Y \left[a_{ij}(y,t) + a_{ik}(y,t)\frac{\partial N_h^j(y,t)}{\partial y_k} \right] \mathrm{d}Y.$$

Therefore, we need to solve the following modified homogenized equation:

$$\begin{cases} \hat{\rho}(t)\dfrac{\partial^2 \tilde{u}^{(0)}(x,t)}{\partial t^2} + \hat{\mu}(t)\dfrac{\partial \tilde{u}^{(0)}(x,t)}{\partial t} \\ = \dfrac{\partial}{\partial x_i}\left(\hat{a}_{ij}^h(t)\dfrac{\partial \tilde{u}^{(0)}(x,t)}{\partial x_j} \right) + f(x,t), \\ (x,t) \in \Omega \times (0,T), \\ \tilde{u}^{(0)}(x,t) = \phi(x,t), \quad (x,t) \in \partial\Omega \times (0,T), \\ \tilde{u}^{(0)}(x,0) = u^0(x), \quad \dfrac{\partial \tilde{u}^{(0)}(x,0)}{\partial t} = u^1(x), \quad x \in \Omega. \end{cases} \tag{44}$$

According to our knowledge, the numerical accuracy of the modified homogenization problem (41) directly affects the accuracy of SOTS. To improve the accuracy of the modified homogenization problem (41), we solve the modified homogenized equation with the quadratic element. Let $J^{h_0} = \{e\}$ be a regular family of triangulation of the spatial region Ω, where $h_0 = \max\{h_e\}$. Define the quadratic finite element space as $V_{h_0} = \{v \in C^0(\Omega) : v\,|_{\partial\Omega} = 0, v\,|_e \in P_2(e)\} \in H_0^1(\Omega)$. Now, we can obtain the semi-discrete scheme for solving problem (51). Firstly, we give the discrete variational formulation for modified homogenization problem (41) as follows:

$$\begin{aligned} &\int_\Omega \hat{\rho}\frac{\partial^2 \tilde{u}_{h_0}^{(0)}}{\partial t^2} v_{h_0}\,\mathrm{d}\Omega + \int_\Omega \hat{\mu}\frac{\partial \tilde{u}_{h_0}^{(0)}}{\partial t} v_{h_0}\,\mathrm{d}\Omega \\ &+ \int_\Omega a_{ij}^h \frac{\partial \tilde{u}_{h_0}^{(0)}}{\partial x_j}\frac{\partial v_{h_0}}{\partial x_i}\,\mathrm{d}\Omega = \int_\Omega f v_{h_0}\,\mathrm{d}\Omega, \\ &\forall v_{h_0} \in V_{h_0}(\Omega), t \in (0,T]. \end{aligned} \tag{45}$$

Secondly, let $\{\phi_i(x)\}_{i=1}^M$ be a basis of V_{h_0} and denote $\tilde{u}_{h_0}^{(0)}(x,t) = \sum_{i=1}^M \xi_i(t)\phi_i(x)$. Then, the discrete variational inequality (42) is equivalent to the following linear ordinary differential system when substituting $\tilde{u}_{h_0}^{(0)}(x,t) = \sum_{i=1}^M \xi_i(t)\phi_i(x)$ into inequality (42):

$$\begin{cases} \boldsymbol{M}(t)\ddot{\boldsymbol{\zeta}}(t) + \boldsymbol{C}(t)\dot{\boldsymbol{\zeta}}(t) + \boldsymbol{K}(t)\boldsymbol{\zeta}(t) = \boldsymbol{Q}(t), \\ \boldsymbol{\zeta}(0) = \boldsymbol{\zeta}^0, \dot{\boldsymbol{\zeta}}(0) = \boldsymbol{\zeta}^1, \end{cases} \tag{46}$$

where $\boldsymbol{\zeta}(t) = [\xi_1(t), \xi_2(t), \ldots, \xi_M(t)]^{\mathrm{T}}$, $\boldsymbol{M}(t), \boldsymbol{C}(t)$, and $\boldsymbol{K}(t)$ are the mass matrix, the damping matrix, and the stiffness matrix, respectively, and $\boldsymbol{Q}(t)$ is the load vector (see Ref. [21]), which can be obtained by the following expressions:

$$\begin{aligned} &\boldsymbol{M}_{ij}(t) = \int_\Omega \hat{\rho}(t)\phi_i\phi_j\,\mathrm{d}\Omega, \boldsymbol{C}_{ij}(t) = \int_\Omega \hat{\mu}(t)\phi_i\phi_j\,\mathrm{d}\Omega, \\ &\boldsymbol{K}_{ij}(t) = \int_\Omega \hat{a}_{ij}^h(t)\phi_i\phi_j\,\mathrm{d}\Omega, \boldsymbol{Q}_i(t) = \int_\Omega f\phi_i\,\mathrm{d}\Omega. \end{aligned} \tag{47}$$

Now, we introduce the Newmark scheme for solving the ordinary differential system (44). As we all know, the Newmark difference scheme is an unconditional stable and convergent difference scheme when scheme parameters $\delta \geq 0.5$ and $\alpha \geq 0.25\,(\delta + 0.5)^2$ (see Refs. [21] and [25]) and we choose $\delta = 0.5$ and $\alpha = 0.25$ in this paper. On the other hand, from Theorem 1, we know that the calculation of SOTS needs the values of acceleration $\partial^2 u^{(0)}/\partial t^2$ and velocity $\partial u^{(0)}/\partial t$ at every time step. The Newmark scheme not only can solve $u^{(0)}$,

but also simultaneously solve $\partial^2 u^{(0)}/\partial t^2$ and $\partial u^{(0)}/\partial t$. So we use the Newmark scheme to solve the ordinary differential system (43) at any time step. The detailed procedure of the Newmark scheme for system (43) is listed as follows.

Step 1 Construct mass matrix $\boldsymbol{M}(t)$, damping matrix $\boldsymbol{C}(t)$, stiffness matrix $\boldsymbol{K}(t)$, and load vector $\boldsymbol{Q}(t)$.

Step 2 Use the initial and boundary conditions $\boldsymbol{\zeta}(0) = \boldsymbol{\zeta}^0$ and $\dot{\boldsymbol{\zeta}}(0) = \boldsymbol{\zeta}^1$ and linear ordinary differential system $\boldsymbol{M}(0)\ddot{\boldsymbol{\zeta}}(0) + \boldsymbol{C}(0)\dot{\boldsymbol{\zeta}}(0) + \boldsymbol{K}(0)\boldsymbol{\zeta}(0) = \boldsymbol{Q}(0)$ to compute the initial $\ddot{\boldsymbol{\zeta}}(0)$.

Step 3 Choose the time step Δt and parameters δ, α. For each time step, we should know $\boldsymbol{\zeta}(t), \dot{\boldsymbol{\zeta}}(t), \ddot{\boldsymbol{\zeta}}(t)$ at first. Then we solve the unknown $\boldsymbol{\zeta}(t+\Delta t)$ by using the following formula (see Ref. [13]):

$$\hat{\boldsymbol{K}}(t+\Delta t)\boldsymbol{\zeta}(t+\Delta t) = \hat{\boldsymbol{Q}}(t+\Delta t), \tag{48}$$

where

$$\begin{aligned}
\hat{\boldsymbol{K}}(t+\Delta t) &= \boldsymbol{K}(t+\Delta t) + \frac{1}{\alpha \Delta t^2}\boldsymbol{M}(t+\Delta t) + \frac{\delta}{\alpha \Delta t}\boldsymbol{C}(t+\Delta t),\\
\hat{\boldsymbol{Q}}(t+\Delta t) &= \hat{\boldsymbol{Q}}(t) + \boldsymbol{M}(t+\Delta t)\left[\frac{1}{\alpha \Delta t^2}\boldsymbol{\zeta}(t) + \frac{1}{\alpha \Delta t}\dot{\boldsymbol{\zeta}}(t) + \left(\frac{1}{2\alpha} - 1\right)\ddot{\boldsymbol{\zeta}}(t)\right]\\
&\quad + \boldsymbol{C}(t+\Delta t)\left[\frac{\delta}{\alpha \Delta t}\boldsymbol{\zeta}(t) + \left(\frac{\delta}{\alpha} - 1\right)\dot{\boldsymbol{\zeta}}(t) + \left(\frac{\delta}{2\alpha} - 1\right)\Delta t\ddot{\boldsymbol{\zeta}}(t)\right].
\end{aligned}$$

Finally, we can derive $\dot{\boldsymbol{\zeta}}(t+\Delta t), \ddot{\boldsymbol{\zeta}}(t+\Delta t)$ by the following formulas:

$$\begin{aligned}
\ddot{\boldsymbol{\zeta}}(t+\Delta t) &= \frac{1}{\alpha \Delta t^2}[\boldsymbol{\zeta}(t+\Delta t) - \boldsymbol{\zeta}(t)] - \frac{1}{\alpha \Delta t}\dot{\boldsymbol{\zeta}}(t) - \left(\frac{1}{2\alpha} - 1\right)\ddot{\boldsymbol{\zeta}}(t),\\
\dot{\boldsymbol{\zeta}}(t+\Delta t) &= \frac{\delta}{\alpha \Delta t}[\boldsymbol{\zeta}(t+\Delta t) - \boldsymbol{\zeta}(t)] + \left(1 - \frac{\delta}{\alpha}\right)\dot{\boldsymbol{\zeta}}(t) + \left(1 - \frac{\delta}{2\alpha}\right)\Delta t\ddot{\boldsymbol{\zeta}}(t).
\end{aligned} \tag{49}$$

Step 4 Repeat step 3 for all time steps, then we can obtain the value of the ordinary differential system (43) at any time step.

4.2. Second-order two-scale numerical method procedure

In this subsection, we present a second-order two-scale numerical method to efficiently solve the hyperbolic–parabolic equations with rapidly oscillating coefficients. Firstly, we give the algorithm of the second-order two-scale numerical method. After that, we give the analysis of SOTS's computational efficiency and superiority to explain why the second-order two-scale numerical method can greatly reduce the calculation compared with the direct finite element method.

Step I Generate a geometric model of the unit cell and compute auxiliary cell functions $N_h^{\alpha_1}(\boldsymbol{y},t), N_h^{\alpha_1\alpha_2}(\boldsymbol{y},t), F_h(\boldsymbol{y},t), G_h(\boldsymbol{y},t)$ on the reference cell $Y = (0,1)^n$ $(n = 2,3)$ by solving the auxiliary cell problems (7) and (12)–(14), respectively.

Step II Calculate the homogenized coefficients $\hat{\rho}(t), \hat{\mu}(t), \hat{a}_{ij}^h(t)$ by taking the integral of Eq. (8). Then solve numerically the modified homogenized hyperbolic–parabolic equation (41) on the whole domain $\Omega \times [0,T]$ with a coarse mesh and a large time step by using the method presented in subsection 4.1.

Step III Solve the spatial variable derivatives $\partial \tilde{u}^{(0)}/\partial x_{\alpha_1}, \partial^2 \tilde{u}^{(0)}/\partial x_{\alpha_1}\partial x_{\alpha_2}$ of the homogenized solutions $\tilde{u}^{(0)}(\boldsymbol{x},t)$ by the average technique on relative elements (see Refs. [2] and [6]) and the temporal variable derivatives $\partial \tilde{u}^{(0)}/\partial t, \partial^2 \tilde{u}^{(0)}/\partial t^2$ by using the difference schemes (46) in subsection 4.1. The following formulas are used for evaluating the high order partial derivatives of the spatial and temporal variables:

$$\frac{\partial \tilde{u}_{h,h_0}^{(0)}}{\partial x_{\alpha_1}}(M,t_i) = \frac{1}{\tau(M)}\sum_{e \in J^{h_0}(M)}\left[\frac{\partial \tilde{u}_{h,h_0}^{(0)}}{\partial x_{\alpha_1}}\right]_e (M,t_i), \tag{50}$$

where M is the node of FEM set J^{h_0}, $J^{h_0}(M)$ denotes the set of elements with the same node M, $\tau(M)$ is the number of elements in $J^{h_0}(M)$, $\left[\partial \tilde{u}_{h,h_0}^{(0)}/\partial x_{\alpha_1}\right]_e (M,t_i)$ denotes the derivative $\partial \tilde{u}_{h,h_0}^{(0)}/\partial x_{\alpha_1}$ at node M on element e and at time $t = t_i$;

$$\begin{aligned}
&\frac{\partial^2 \tilde{u}_{h,h_0}^{(0)}}{\partial x_{\alpha_1}\partial x_{\alpha_2}}(M,t_i)\\
&= \frac{1}{\tau(M)}\sum_{e \in J^{h_0}(M)}\left[\sum_{j=1}^{m}\frac{\partial \tilde{u}_{h,h_0}^{(0)}(p_j,t_i)}{\partial x_{\alpha_1}}\cdot\frac{\partial \phi_j^e(\boldsymbol{x})}{\partial x_{\alpha_2}}\right]_e (M,t_i),
\end{aligned} \tag{51}$$

where m is the number of node freedom on element e, and $\phi_j^e(\boldsymbol{x})$ is the Lagrange's type shape function corresponding to node p_j on e;

$$\begin{aligned}
&\frac{\partial^2 \tilde{u}_{h,h_0}^{(0)}}{\partial t^2}(M,t_i)\\
&= \ddot{\zeta}_M(t_i) = \frac{1}{\alpha \Delta t^2}(\zeta_M(t_i) - \zeta_M(t_{i-1})) - \frac{1}{\alpha \Delta t}\dot{\zeta}_M(t_{i-1}) - \left(\frac{1}{2\alpha} - 1\right)\ddot{\zeta}_M(t_{i-1}),
\end{aligned} \tag{52}$$

$$\begin{aligned}
&\frac{\partial \tilde{u}_{h,h_0}^{(0)}}{\partial t}(M,t_i)\\
&= \dot{\zeta}_M(t_i) = \frac{\delta}{\alpha \Delta t}(\zeta_M(t_i) - \zeta_M(t_{i-1})) + \left(1 - \frac{\delta}{\alpha}\right)\dot{\zeta}_M(t_{i-1}) + \left(1 - \frac{\delta}{2\alpha}\right)\Delta t\ddot{\zeta}_M(t_{i-1}),
\end{aligned} \tag{53}$$

where $\zeta_M(t_i)$ denotes the value of node M at time $t = t_i$, $\dot{\zeta}_M(t_i), \ddot{\zeta}_M(t_i)$ are the first-order and the second-order partial derivatives of the temporal variables at time $t = t_i$.

Step IV Use the auxiliary cell functions in step 1 to assemble SOTS as follows:

$$\begin{aligned} u_{h,h_0}^{(2\varepsilon)}(M,t_i) &= \tilde{u}_{h,h_0}^{(0)}(M,t_i)+\varepsilon N_h^{\alpha_1}(t_i)\frac{\partial \tilde{u}_{h,h_0}^{(0)}}{\partial x_{\alpha_1}}(M,t_i)\\ &\quad+\varepsilon^2 N_h^{\alpha_1\alpha_2}(t_i)\frac{\partial^2 \tilde{u}_{h,h_0}^{(0)}}{\partial x_{\alpha_1}\partial x_{\alpha_2}}(M,t_i)\\ &\quad+\varepsilon^2 F_h(t_i)\frac{\partial^2 \tilde{u}_{h,h_0}^{(0)}}{\partial t^2}(M,t_i)\\ &\quad+\varepsilon^2 G_h(t_i)\frac{\partial \tilde{u}_{h,h_0}^{(0)}}{\partial t}(M,t_i). \end{aligned} \tag{54}$$

Step V For arbitrary point $(\boldsymbol{x},t)\in\Omega\times[0,T]$, we use the higher-order interpolation method to obtain the high-precision SOTS value as follows:

$$\begin{aligned} u_{h,h_0}^{(2\varepsilon)}(\boldsymbol{x},t) &= \tilde{u}_{h,2h_0}^{(0)}(\boldsymbol{x},t)+\varepsilon N_{2h}^{\alpha_1}(t)\frac{\partial \tilde{u}_{h,2h_0}^{(0)}}{\partial x_{\alpha_1}}(\boldsymbol{x},t)\\ &\quad+\varepsilon^2 N_{2h}^{\alpha_1\alpha_2}(t)\frac{\partial^2 \tilde{u}_{h,2h_0}^{(0)}}{\partial x_{\alpha_1}\partial x_{\alpha_2}}(\boldsymbol{x},t)\\ &\quad+\varepsilon^2 F_{2h}(t)\frac{\partial^2 \tilde{u}_{h,2h_0}^{(0)}}{\partial t^2}(\boldsymbol{x},t)\\ &\quad+\varepsilon^2 G_{2h}(t)\frac{\partial \tilde{u}_{h,2h_0}^{(0)}}{\partial t}(\boldsymbol{x},t), \end{aligned} \tag{55}$$

where

$$\begin{aligned} &\tilde{u}_{h,2h_0}^{(0)}(\boldsymbol{x},t)\\ &= l(t)\mathcal{I}_{2h_0}^{2r}\tilde{u}_{h,h_0}^{(0)}(\boldsymbol{x},t_i)+(1-l(t))\mathcal{I}_{2h_0}^{2r}\tilde{u}_{h,h_0}^{(0)}(\boldsymbol{x},t_{i-1}),\\ &t\in[t_{i-1},t_i],\quad 0=t_0<t_1<\cdots<t_N=T,\\ &l(t)=\frac{(t-t_i)}{\Delta t_i},\quad \Delta t_i=t_i-t_{i-1},\\ &\frac{\partial^2 \tilde{u}_{h,2h_0}^{(0)}}{\partial t^2}(\boldsymbol{x},t)\\ &= l(t)\left[\mathcal{I}_{2h_0}^{2r}\frac{\partial^2 \tilde{u}_{h,h_0}^{(0)}}{\partial t^2}\right](\boldsymbol{x},t_i)+(1-l(t))\left[\mathcal{I}_{2h_0}^{2r}\frac{\partial^2 \tilde{u}_{h,h_0}^{(0)}}{\partial t^2}\right](\boldsymbol{x},t_{i-1}),\\ &\frac{\partial \tilde{u}_{h,2h_0}^{(0)}}{\partial t}(\boldsymbol{x},t)\\ &= l(t)\left[\mathcal{I}_{2h_0}^{2r}\frac{\partial \tilde{u}_{h,h_0}^{(0)}}{\partial t}\right](\boldsymbol{x},t_i)+(1-l(t))\left[\mathcal{I}_{2h_0}^{2r}\frac{\partial \tilde{u}_{h,h_0}^{(0)}}{\partial t}\right](\boldsymbol{x},t_{i-1}), \end{aligned}$$

$N_{2h}^{\alpha_1}=\mathcal{I}_{2h}^{2r}N_h^{\alpha_1}$, $N_{2h}^{\alpha_1\alpha_2}$, F_{2h}, G_{2h} likeness,

$$N_{2h}^{\alpha_1}(t)=l(t)N_{2h}^{\alpha_1}(t_i)+(1-l(t))N_{2h}^{\alpha_1}(t_{i-1}),$$

$N_{2h}^{\alpha_1\alpha_2}(t)$, $F_{2h}(t)$, $G_{2h}(t)$ likeness, and the higher-order interpolation operator $\mathcal{I}_{2h_0}^{2r}$ and $\mathcal{I}_{2h}^{2r}$ can be found in Refs. [2]–[7] and [26].

The main motivation to develop multiscale methods is to solve the problems which cannot be solved by the conventional numerical methods. So the analysis of the computational efficiency of multiscale methods only can be done when we assume that the multiscale problems can be solved by the conventional numerical methods. Firstly, we give a specific analysis to explain why the SOTS can greatly reduce computational cost compared with the direct FEM. We assume that the whole domain Ω consists of $n\times n$ entire periodic cells. If we need m elements to mesh every unit cell in Ω, the total number of elements is $n\times n\times m$ in the direct FEM calculation. Fortunately, SOTS only needs the grid information of a single cell to solve the auxiliary cell problems. From Section 2, we know that there are two auxiliary cell problems $N^{\alpha_1}(\boldsymbol{y},t)$, four $N^{\alpha_1\alpha_2}(\boldsymbol{y},t)$, one $F(\boldsymbol{y},t)$, and one $G(\boldsymbol{y},t)$ for the two-dimensional hyperbolic–parabolic equations. Thus, the total number of elements to solve the auxiliary cell problems is $8m$. Luckily, this number does not increase even if the cell number of the whole domain Ω increases. On the other hand, we assume that the elements for solving the homogenization problem is $c\times n\times n\times m(0<c\ll 1)$. In the general calculation, c is in the range from $1/20$ to $1/5$ (see Refs. [3]–[7], and [11]). In summary, the total element number of SOTS is $\left(cn^2+8m\right)$ at every time step. With the rapid increase of cell number $n\times n$, it is easy to know SOTS can save $19/20$–$4/5$ of the elements in the two-dimensional hyperbolic–parabolic equations. By a similar analysis, we know that SOTS for the three-dimensional equations still can save $19/20$–$4/5$ of the elements. So one can understand why SOTS can greatly reduce the computing resources and improve the computational efficiency.

Now, we give a detailed analysis of the SOTS's stability. Due to the great difference of material coefficients between different kinds of materials in the composite structure, if we use the finite element method to solve problem (1) directly, the overall damping matrix and stiffness matrix are ill-conditioned matrices. Although they are all symmetric definite matrices, the difference between the maximum eigenvalue and the minimum eigenvalue of the overall damping matrix and the stiffness matrix is too big. So the numerical results will be unstable, which causes a larger error. Fortunately, if we use SOTS to solve problem (1), the overall damping matrix and the stiffness matrix have good properties because the homogenized material coefficients of homogenization problem (41) are functions which vary slowly. Therefore, the numerical algorithms we presented have good stability compared with the direct FEM. At the same time, we can use a large time step to solve homogenization problem (41) because the overall damping matrix and the stiffness matrix are both well-conditioned matrices.

5. Numerical tests

Example 1 In this example, we verify our algorithms for problem (1) in which the material coefficients are all time-independent in the two-dimensional situation and we denote

this case as case 1. Here Y_1 represents the matrix and Y_2 represents inclusions in the composite structure. Besides, we let the size ε of the periodic cell equal to $1/10$. The material coefficients are

$$\rho(\boldsymbol{y}) = \begin{cases} 1, \text{ in } Y_1, \\ 0.5, \text{ in } Y_2, \end{cases} \quad \mu(\boldsymbol{y}) = \begin{cases} 10, \text{ in } Y_1, \\ 5, \text{ in } Y_2, \end{cases}$$

$$a_{ij}(\boldsymbol{y}) = \begin{cases} \delta_{ij}, \text{ in } Y_1, \\ 0.01\delta_{ij}, \text{ in } Y_2. \end{cases} \tag{56}$$

The undefined functions in problem (1) are

$$f(\boldsymbol{x},t) = 0, \ \ \phi(\boldsymbol{x},t) = 0,$$
$$u^0(\boldsymbol{x}) = xy(x-1)(y-1), \ \ u^1(\boldsymbol{x}) = 0. \tag{57}$$

Table 1. Comparison of computational cost ($\Delta t = 0.005$, $t \in [0,5]$).

	Original equation	Cell problem	Homogenized equation
Number of elements	88200	3438	1450
Number of nodes	44501	1800	776
Computational time/s	3773.8	728.265	

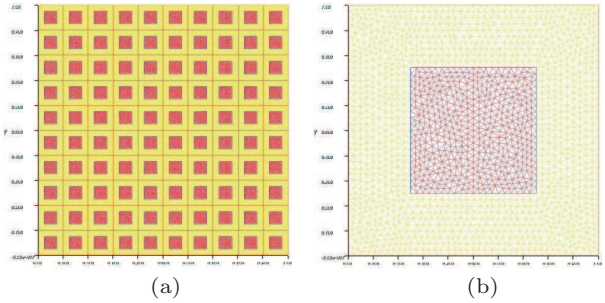


Fig. 2. (color online) (a) The whole domain Ω and (b) the unit cell Y of case 1.

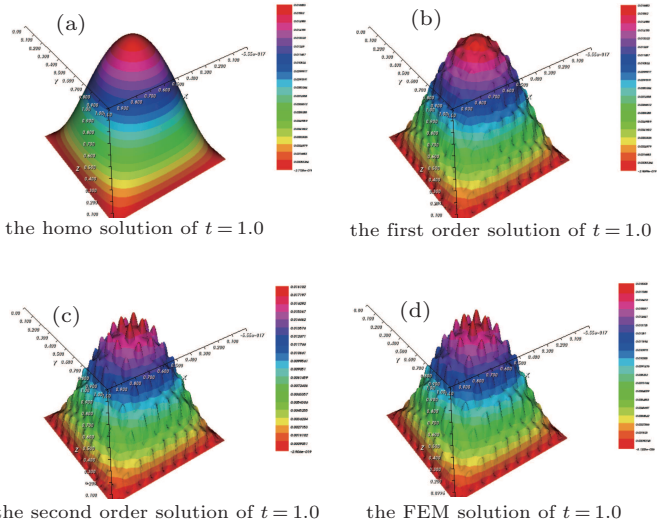


Fig. 3. (color online) (a) $u^{(0)}$, (b) $u^{(1\varepsilon)}$, (c) $u^{(2\varepsilon)}$, and (d) u^{ε} of case 1 at $t = 1.0$.

As is known to all, problem (1) does not have any analytical solution. We denote fine FEM as u^{ε}. From Table 1, it is easy to see that SOTS can greatly reduce the computational time. Figures 3 and 4 show the numerical results of $u^{(0)}$, $u^{(1\varepsilon)}$, $u^{(2\varepsilon)}$, and u^{ε} at time $t = 1.0$ and $t = 3.0$, respectively. From Figs. 3 and 4, one can find that only SOTS can accurately capture the micro-scale oscillating information and FOTS is far from enough to obtain the high accuracy solution. In Fig. 5, the damping decay behavior of point (0.45,0.45) is shown. One can clearly see that SOTS and u^{ε} fit perfectly. Figure 6 shows that whether it is the L^2 norm or the H^1 norm, the accuracy of SOTS is much better than FOTS and the homogenized solution. Especially for the H^1 norm, SOTS has more advantages. In practical engineering applications, engineers are more concerned about the gradient of u^{ε} because the gradient represents the flux or strain.

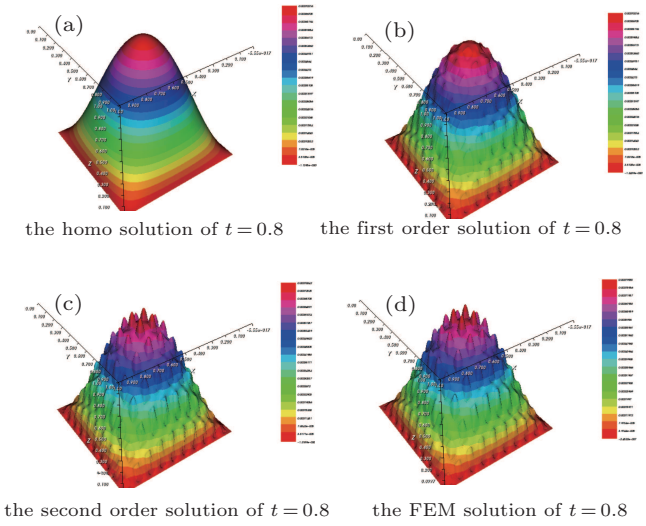


Fig. 4. (color online) (a) $u^{(0)}$, (b) $u^{(1\varepsilon)}$, (c) $u^{(2\varepsilon)}$, and (d) u^{ε} of case 1 at $t = 3.0$.

Remark 4 From Figs. 5 and 6, one can see that there is a bigger difference between the solution of SOTS and the fine FEM in a very short time at the beginning of the calculation. This phenomenon is because SOTS is used to capture the micro-scale fluctuation information due to the heterogeneities, but in fact the exact solutions of problem (1) do not have severe fluctuations due to the damping at the beginning. This situation is easy to handle. For example, we can use FOTS to replace SOTS or abandon the term $N^{\alpha_1\alpha_2}\frac{\partial^2 u^{(0)}}{\partial x_{\alpha_1}\partial x_{\alpha_2}}$ of SOTS in a short time at the beginning. In addition, the error increases with time, this is because the reliability of the fine finite element solution decreases when the time goes forward.

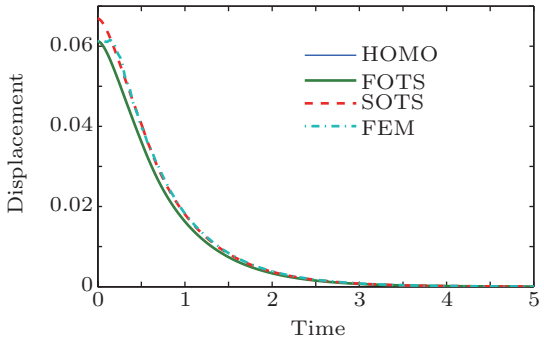


Fig. 5. (color online) The damping behavior of point (0.45, 0.45) in case 1.

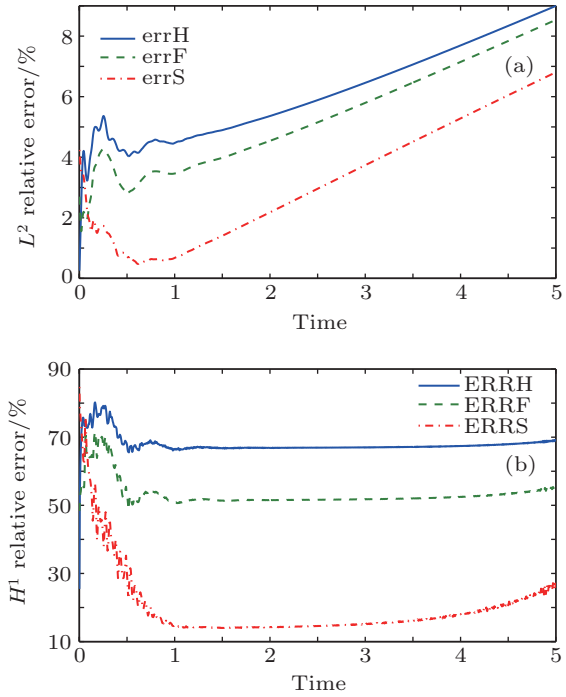


Fig. 6. (color online) (a) L^2 relative error and (b) H^1 relative error of case 1.

Remark 5 Notably, we use a small time step $\Delta t = 0.005$ in the above calculation. This is only for the computational stability of the fine FEM which is needed in the error analysis. In fact, our second-order two-scale algorithm can take a large time step in practical computations and still be stable.

Example 2 In this example, we verify our algorithms for problem (1) in which the material coefficients are all time-dependent in the two-dimensional situation and we denote this case as case 2. The definitions of Y_1, Y_2, and ε are the same as those in example 1. The material coefficients are

$$\rho(\boldsymbol{y},t) = \begin{cases} 1\,\mathrm{e}^{-0.105t}, & \text{in } Y_1, \\ 0.5\,\mathrm{e}^{-0.105t}, & \text{in } Y_2, \end{cases}$$

$$\mu(\boldsymbol{y},t) = \begin{cases} 10\,\mathrm{e}^{-0.105t}, & \text{in } Y_1, \\ 5\,\mathrm{e}^{-0.105t}, & \text{in } Y_2, \end{cases}$$

$$a_{ij}(\boldsymbol{y},t) = \begin{cases} \mathrm{e}^{-0.105t}\delta_{ij}, & \text{in } Y_1, \\ 0.01\,\mathrm{e}^{-0.105t}\delta_{ij}, & \text{in } Y_2. \end{cases} \tag{58}$$

The undefined functions in equations (1) are

$$f(\boldsymbol{x},t) = 0, \quad \phi(\boldsymbol{x},t) = 0,$$

$$u^0(\boldsymbol{x}) = xy(x-1)(y-1), \quad u^1(\boldsymbol{x}) = 0. \tag{59}$$

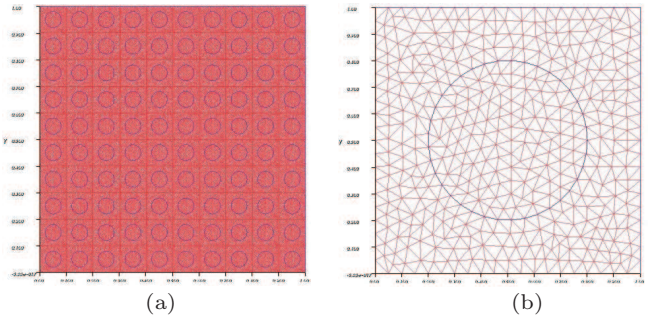


Fig. 7. (color online) (a) The whole domain Ω and (b) the unit cell Y of case 2.

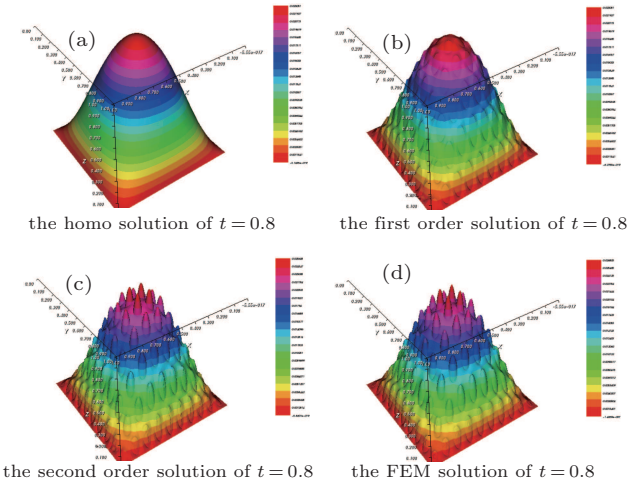


Fig. 8. (color online) (a) $u^{(0)}$, (b) $u^{(1\varepsilon)}$, (c) $u^{(2\varepsilon)}$, and (d) u^{ε} of case 2 at $t = 0.8$.

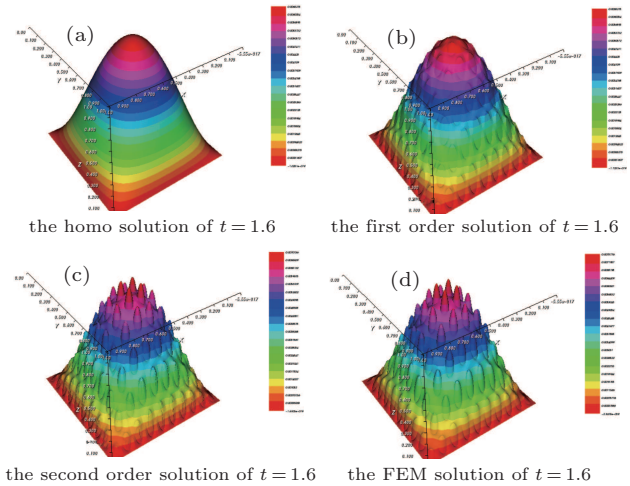


Fig. 9. (color online) (a) $u^{(0)}$, (b) $u^{(1\varepsilon)}$, (c) $u^{(2\varepsilon)}$, and (d) u^{ε} of case 2 at $t = 1.6$.

From Table 2, it is easy to see that SOTS still can greatly reduce the computational time. Figures 8 and 9 show the numerical results at time $t = 0.8$ and $t = 1.6$. From these two figures, one can find that only SOTS can accurately

Table 2. Comparison of computational cost ($\Delta t = 0.002$, $t \in [0,2]$).

	Original equation	Cell problem	Homogenized equation
Number of elements	83600	836	1450
Number of nodes	42201	459	776
Computational time/s	3689.43		914.542

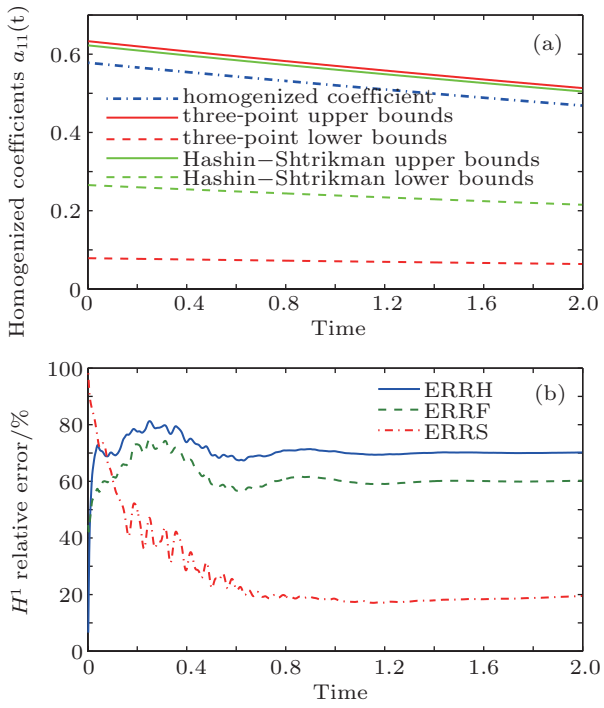


Fig. 10. (color online) (a) $\hat{a}_{11}(t)$ and (b) H^1 relative error of case 2.

capture the oscillating information in the micro scale and FOTS cannot obtain the high accuracy solution of multiscale problem (1). In Fig. 10(a), the dynamic homogenized coefficient $\hat{a}_{11}(t)$ is shown. One can find that homogenized coefficient $\hat{a}_{11}(t)$ falls between the upper bound and the lower bound of the Hashin–Shtrikman bounds and the three-point bounds at every time step. Figure 10(b) shows that the accuracy of SOTS is much better than FOTS and the homogenized solution in the H^1 norm sense.

6. Conclusion

We discuss the second-order two-scale analysis and multiscale numerical algorithms for the hyperbolic–parabolic equations with rapidly oscillating coefficients. The new contributions of this paper include the second-order two-scale analysis, the determination of the SOTS's convergence rate under some assumptions, and the corresponding second-order two-scale numerical method. Numerical experiments show that the multiscale numerical algorithm we proposed is stable and efficient. Furthermore, the numerical results show that only SOTS can accurately capture the micro-scale oscillating information of multiscale problem (1).

References

[1] Wu Y T, Nie Y F and Yang Z H 2014 *CMES-Computer Modeling in Engineering & Sciences* **4** 297

[2] Cui J Z 2001 *Proceedings on Computational Mechanics in Science and Engineering*, Peking University Press, December 5–8, 2001, Guangzhou, China, p. 33

[3] Yang Z Q, Cui J Z and Li B W 2014 *Chin. Phys. B* **23** 030203

[4] Su F, Cui J Z, Xu Z and Dong Q L 2010 *Finite Elements in Analysis and Design* **46** 320

[5] Cao L Q, Cui J Z and Luo J L 2003 *Journal of Computational and Applied Mathematics* **157** 1

[6] Dong Q L and Cao L Q 2014 *Applied Mathematics and Computation* **232** 872

[7] Dong Q L and Cao L Q 2009 *Applied Numerical Mathematics* **59** 3008

[8] Cao L Q 2005 *Numerische Mathematik* **103** 11

[9] Cao L Q, Cui J Z and Zhu D C 2002 *SIAM Journal on Numerical Analysis* **40** 543

[10] Cao L Q and Cui J Z 2004 *Numerische Mathematik* **96** 525

[11] Yang Z H, Chen Y, Yang Z Q and Ma Q 2014 *Chin. Phys. B* **23** 076501

[12] Migórski S 1996 *Universitatis Iagellonicae Acta Matematica* **33** 59

[13] Nguetseng G, Nnang H and Svanstedt N 2010 *Journal Of Function Spaces And Applications* **8** 17

[14] Lu L Q and Li S J 2014 *Journal of Mathematical Analysis and Applications* **418** 64

[15] Zhang S 2007 *Thermodynamic Analysis of Periodic MultiPhase Materials by Spatial and Temporal Multiscale Method* (Ph. D. Dissertation) (Dalian: Dalian University of Technology) (in Chinese)

[16] Timofte C 2010 *AIP Conference Proceedings* **1301** 543

[17] Hubert N 2012 *Nonlinear Differential Equations and Applications NoDEA* **19** 539

[18] Narazaki T 2004 *J. Math. Soc* **56** 585

[19] Radu P, Todorova G and Yordanov B 2010 *Trans. Amer. Math. Soc* **362** 2279

[20] Todorova G and Yordanov B 2009 *J. Differential Equations* **246** 4497

[21] Zhang X and Wang T S 2007 *Computational Dynamics* (Beijing: Tsinghua University press) (in Chinese) pp. 162–167

[22] Bensoussan A, Lions J L and Papanicolaou G 1978 *Asymptotic Analysis of Periodic Structures* (Amsterdam: North-Holland Publishing Company) pp. 537–545

[23] Oleinik O A, Shamaev A S and Yosifian G A 1992 *Mathematical Problems in Elasticity and Homogenization* (Amsterdam: North-Holland Publishing Company) pp. 13–23

[24] Cioranescu D and Donato P 1999 *An Introduction to Homogenization* (New York: Oxford University Press) pp. 125–137, 222–238

[25] Braess D 2007 *Finite Elements Theory, Fast Solvers, and Applications in Elasticity Theory* (Cambridge: Cambridge University Press)

[26] Lin Q and Zhu Q D 1994 *The Preprocessing snd Preprocessing for the Finite Element Method* (Shanghai: Shanghai Scientific & Technical Publishers) (in Chinese) pp. 57–65